JOURNAL OF COMPUTATIONAL PHYSICS **133,** 256–278 (1997)
ARTICLE NO. CP975660

A Numerical Method for the Computation of the Dispersion of a Cloud of Particles by a Turbulent Gas Flow Field

K. Domelevo[1] and L. Sainsaulieu[2]

Centre de Mathématiques Appliquées, Ecole Polytechnique, 91128 Palaiseau Cedex, France; and, CERMICS, ENPC, Central 2, La Courtine, 93167 Noisy-le-Grand Cedex, France.

Received May 30, 1996; revised January 29, 1997

The paper is concerned with the construction of a numerical method for the computation of the dispersion of a cloud of liquid droplets by a turbulent gas flow field. The cloud of droplets is modeled by a semi-fluid system intermediate between a fluid model and a kinetic description of the dispersed phase. The semi-fluid model is deduced from the kinetic model by integration with respect to the velocity variables and makes it possible to describe clouds of particles such that the velocity distribution of any family of particles with a given radius and a given temperature found at a given location of the physical space is a Gaussian function. A numerical scheme, consistent with the semi-fluid model and inspired by Perthame's or Deshpande's kinetic schemes, is proposed. The interactions with the gas phase are taken into account thanks to a particle in cell method. Numerical experiments illuminate the features of the method.

1. INTRODUCTION

This work deals with the numerical simulation of vaporizing two-phase fluid flows consisting of a spray of liquid droplets in a surrounding turbulent hot gas flow. The prediction of the turbulent induced mixing of the cloud of droplets is of primary importance in the simulation of Diesel engines, for instance. In such devices, liquid fuel is injected into the combustion chamber at high pressure, which causes breakup of the liquid core and formation of small droplets. In this study we do not consider the atomization of fuel, which is still an open problem from the numerical viewpoint. On the contrary, we propose a numerical method for the computation of the dispersion of a dilute spray by a turbulent gas flow field. We shall thus assume no interactions between droplets such as breakup or collisions. Nevertheless, the mass of droplets in practical devices such as Diesel engines is of the same order as the mass of gas and one should take into account the exchanges of mass, momentum, and of course energy between the two phases. However, for the sake of simplicity, we do not introduce combustion models in this work but only consider vaporization of droplets since our main interest lies in the prediction of the dispersion of the cloud of droplets. This study is thus a preliminary step towards the computation of the full piston in a Diesel engine.

In order to model two-phase fluid flows, we might either chose an Eulerian model or a Lagrangian one. In the Eulerian approach, each phase is modeled as a single fluid, occupying the whole physical space. Exchange terms are included to account for the exchanges of mass, momentum, and energy between the two phases. Such models are usually obtained by averaging the Navier–Stokes equations satisfied by the gas phase around the droplets and the liquid phase inside the droplets. Since the location of the droplets may change from one experiment to another one, this method defines mean quantities that characterize the two-phase flow, which are defined in the whole physical space. Nevertheless, the derivation of such models is usually tricky and requires many assumptions on the velocity and radius distributions of the cloud of droplets. Furthermore, the numerical treatment of Eulerian models is usually a difficult task which requires much work and the numerical results often poorly compare with experimental results. On the contrary, physical laws are easily included in Lagrangian models. Here droplets are characterized by their position in the phase space and the modeling stage consists in writing the droplets trajectory in the phase space. Here the description of the motion of the droplets may be as complicated as necessary. The interaction with the gas phase is taken into account through correlations: the regression velocity of a droplet's radius may depend for instance on the temperature and on the velocity of the gas around the droplet. In the same manner production terms are included in the gas phase equation so as to ensure the global conservation of mass, momentum and energy of the two-phase flow. Note that alternately, using Liouville's

[1] E-mail: komla@cmapx.polytechnique.fr.
[2] E-mail: sainsau@cmapx.polytechnique.fr.

0021-9991/97 $25.00

theorem, the Lagrangian model may be written in the form of a kinetic one that gives the evolution of the probability density function of the cloud of particles. This equation is also known as the spray equation (see [1] for more details).

Writing a Lagrangian model is thus much easier than writing an Eulerian one. But two-phase flow experiments typically involve 10^6—10^{10} particles and it is of course impossible to compute so many particles. Furthermore, we are not interested in the precise locations of particles but in average behavior. The usual trick is to consider numerical particles which represent a group of particles with the same velocity and the same radius at a given location of the phase space. Provided that the velocity and droplet distributions of the cloud are smooth enough, this method is efficient and enables the computation of Lagrangian models. However, such computations still require much CPU time due to the great number of numerical particles that should be computed in order to obtain meaningful results. Furthermore, in the case of the dispersion of a cloud by a isotropic and homogeneous turbulent gas flow field, [2] proves that the velocity distribution of a class of particles of given radius and at a given location of the physical space asymptotically tends to a Gaussian distribution. Assuming that the last velocity distribution functions are Gaussian, we introduce below a semi-fluid model where each class of droplets with a given radius and found at a given location of the phase space is characterized by its number density, its mean velocity, and its mean quadratic velocity. The semi-fluid model is derived by taking the first three moments of the spray equation relative to the velocity variable. The semi-fluid model consists of three equations, written in a space with dimension 4 (the three position variables and the radius), while the spray equation is a single equation written in a phase space with dimension 7. The semi-fluid description of the two-phase flow thus requires many fewer degrees of freedom than the Lagrangian description and we expect much more efficient computer codes based on this model than on fully Lagrangian models without sacrificing for a precise description of the behavior of droplets.

We introduce in this paper a numerical method for the computation of our semi-fluid model. The method is inspired by the kinetic schemes of Harten, Desphande, and Perthame (see [3–5]) and relies on the spray equation. Nevertheless the semi-fluid model is written in a space with dimension 4 and we resort to a particle description of the unknown functions rather than to a finite volume approach as in the work of Perthame. The organization of the paper is the following: Section **2** is devoted to the derivation of the semi-fluid model from the spray equation. Section **3** deals with the discretization of the semi-fluid model. A finite volume method for the computation of the gas phase and the treatment of the interaction between the gas and the liquid phase thanks to a particle in cell method is proposed in Section **4**. Numerical results are shown in Section **5**.

2. MODELING

2.1. *A Kinetic Model*

In the kinetic approach, the particles are characterized by their position in the phase space, namely by their position $\mathbf{x}$, their velocity $\mathbf{v}$, and their radius r. We do not take the temperature into account here. The corresponding probability density function (pdf) is then a function $f = f(\mathbf{x}, \mathbf{v}, r, t)$ and the spray equation is written (see [1, 6]):

$$\partial_t f + \nabla_{\mathbf{x}} \cdot (f\mathbf{v}) + \nabla_{\mathbf{v}} \cdot (f\beta) + \partial_{\mathbf{r}}(f\mathscr{R}) = Q(f, f). \qquad (2.1)$$

The term $\beta = \beta(\mathbf{x}, \mathbf{v}, r, t)$ is the acceleration of a droplet with velocity $\mathbf{v}$ and radius r, at time t. The term $\mathscr{R}$ is the regression velocity of the radius of the droplets:

$$\mathscr{R} = \frac{dr}{dt}.$$

This term takes into account the vaporization of the droplets. There exist many models accounting for this phenomenon. Here, for the sake of simpliciy, we shall assume that when a droplet vaporizes its radius obeys the so called d^2-law: $r^2(t) = r_0^2 - Kt$, where K is a positive constant (see [1]). This means that $\mathscr{R} = -K/2r$. When using this simple model, one assumes that the temperature inside the droplet is constant and uniform and that the surrounding gas is still. These are reliable assumptions when there exists a certain equilibrium between the vaporizing droplet and the surrounding gas. These assumptions are not verified in most practical cases but we may use the d^2-law when the droplets are injected in a hot gas so that the temperature of the droplets reaches the boiling point in a short time compared to the time for the complete vaporization of the droplet. Hence, as a preliminary step toward more realistic models, we may omit the droplet temperature in the pdf by assuming that this temperature equals the boiling temperature of the liquid inside the droplets. Finally, $Q(f, f)$ is a nonlinear expression that takes into account the collisions of particles and the break-up. In the sequel, we consider dilute clouds of particles, so that we omit the term $Q(f, f)$ in (2.1). The spray equation reduces to the transport equation in the phase space:

$$\partial_t f + \nabla_{\mathbf{x}} \cdot (f\mathbf{v}) + \nabla_{\mathbf{v}} \cdot (f\beta) + \partial_r(f\mathscr{R}) = 0. \qquad (2.2)$$

The acceleration β of a droplet includes the drag force, the acceleration of gravity, the added mass effect, the Basset term, ... In this study we shall only take into account

the drag force and the gravity force, which are the two leading forces that act on droplets. The term β is thus

$$\beta = \beta_s + \mathbf{g}$$

where $\mathbf{g}$ is the acceleration of gravity and β_s is the drag acceleration. Here, for the sake of simplicity and without loss of generality in the sequel, we set $\mathbf{g} \equiv 0$. Finally, we model the drag acceleration by the Stokes drag force:

$$\beta_s = -\frac{9}{2}\frac{\mu_g}{r^2\rho_l}(\mathbf{v} - \mathbf{u}_g) = -c(r)(\mathbf{v} - \mathbf{u}_g) = -\frac{\mathscr{C}}{r^2}(\mathbf{v} - \mathbf{u}_g). \tag{2.3}$$

Here, μ_g denotes the viscosity of the gas, ρ_l is the mass density of the liquid phase, and $\mathbf{u}_g$ is the velocity of the gas. We assume below that μ_g and ρ_l are positive constants. Hence, the action of the gas on the particles occurs through the acceleration β_s, which depends on $\mathbf{u}_g$. Furthermore, when the velocities of the gas and of the droplets are large, the effects of gravity may be neglected and we set $\mathbf{g} = 0$ in the sequel. Finally, note that $1/c(r)$ is the characteristic relaxation time for a droplet with radius r to be captured by the gas flow, i.e., the time after which the velocity of the droplet equals that of the surrounding gas.

The gas flow field is modeled by the Navier–Stokes equations:

$$\begin{cases} \partial_t(\rho_g) + \nabla_{\mathbf{x}} \cdot (\rho_g \mathbf{u}_g) = \mathbf{M} \\ \partial_t(\rho_g \mathbf{u}_g) + \nabla_{\mathbf{x}} \cdot (\rho_g \mathbf{u}_g \otimes \mathbf{u}_g + p_g I) - \nabla_{\mathbf{x}} \cdot (\sigma_g') = \mathbf{I} \\ \partial_t(\rho_g e_g) + \nabla_{\mathbf{x}} \cdot (\rho_g e_g \mathbf{u}_g + p_g \mathbf{u}_g) - \nabla_{\mathbf{x}} \cdot (\sigma_g' \cdot \mathbf{u}_g) \\ \qquad\qquad - \nabla_{\mathbf{x}} \cdot (\kappa_g \nabla_{\mathbf{x}} \varepsilon_g) = \mathbf{E}. \end{cases} \tag{2.4}$$

The functions p_g, ε_g, κ_g and σ_g' are respectively the pressure, the specific internal energy, the gas thermal conductivity, and the viscous stress tensor of the gas. Their expressions are given by the formulae

$$\begin{aligned} \varepsilon_g &= e_g - \frac{\mathbf{u}_g^2}{2} \\ p_g &= (\gamma - 1)\rho_g \varepsilon_g = (\gamma - 1)\rho_g \left(e_g - \frac{\mathbf{u}_g^2}{2} \right) \\ \sigma_g' &= \mu_g(\nabla_{\mathbf{x}} \mathbf{u}_g + \nabla_{\mathbf{x}} \mathbf{u}_g^{\mathrm{T}}) + \lambda(\nabla_{\mathbf{x}} \cdot \mathbf{u}_g) I, \end{aligned} \tag{2.5}$$

where γ is the ratio of specific heats, μ_g is the gas viscosity, and λ is the bulk viscosity.

The exchange terms $\mathbf{M}$, $\mathbf{I}$, and $\mathbf{E}$ in (2.4) are such that the total mass, momentum and energy of the system are conserved; that is,

$$\begin{aligned} &\partial_t \int_{\mathbf{v}} \int_r f \frac{4}{3}\pi r^3 \rho_l \left[1, \mathbf{v}, \frac{\mathbf{v}^2}{2} \right] d\mathbf{v}\, dr + \nabla_{\mathbf{x}} \\ &\qquad \cdot \left(\int_{\mathbf{v}} \int_r f \mathbf{v} \phi(\mathbf{v}, r)\, d\mathbf{v}\, dr \right) \stackrel{\text{def}}{=} -[\mathbf{M}, \mathbf{I}, \mathbf{E}](x, t), \end{aligned} \tag{2.6}$$

which yields the expressions

$$\begin{cases} \mathbf{M}(\mathbf{x}, t) = \displaystyle\int_r 2K\pi\rho_l r\, dr \int_{\mathbf{v}} f\, d\mathbf{v} \\ \mathbf{I}(\mathbf{x}, t) = \displaystyle\int_r 2K\pi\rho_l r\, dr \int_{\mathbf{v}} f\mathbf{v}\, d\mathbf{v} \\ \qquad\qquad - \displaystyle\int_r c(r)\frac{4}{3}\pi\rho_l r^3\, dr \int_{\mathbf{v}} f(\mathbf{u}_g - \mathbf{v})\, d\mathbf{v} \\ \mathbf{E}(\mathbf{x}, t) = \displaystyle\int_r 2K\pi\rho_l r\, dr \int_{\mathbf{v}} f\frac{\mathbf{v}^2}{2} d\mathbf{v} \\ \qquad\qquad - 2\displaystyle\int_r c(r)\frac{4}{3}\pi\rho_l r^3\, dr \int_{\mathbf{v}} f(\mathbf{u}_g - \mathbf{v}) \cdot \mathbf{v}\, d\mathbf{v}. \end{cases} \tag{2.7}$$

2.2. *Turbulence Modeling*

Let us now consider the modeling of the turbulence in the two-phase flow. The equations written above indeed allow direct simulation of the turbulent two-phase flow. Nevertheless, direct simulation requires that the mesh size be much smaller than the size of the smallest eddies. But since eddies are expected in the wake of droplets, the mesh size should be much smaller than the droplet radius in order to perform direct simulation of the two-phase flow. Hence, practical computations using direct simulation would only allow very few droplets and we need turbulence modeling.

The modeling of turbulence in two-phase flows is still an open problem and we expect that the presence of droplets perturbs Kolmogorov's energy cascade. Here, we distinguish two scales for the turbulent eddies. On the one hand, in the "macroscopic scale," we consider that the eddies are big enough so that the turbulence phenomenon may be included in the description of the mean velocity of the gas. Hence, we may write here the velocity of the gas as the sum (see [7, 8])

$$\mathbf{u}_g = \overline{\mathbf{u}_g} + \tilde{\mathbf{u}}, \tag{2.8}$$

where $\overline{\mathbf{u}_g}$ is mean velocity in the statistical sense and $\tilde{\mathbf{u}}$ is modeled by a centered random fluctuation. The value of $\tilde{\mathbf{u}}$ depends on the turbulent kinetic energy of the gas and acts on the droplets during the turbulence correlation time τ. When $\tilde{\mathbf{u}}$ is modelled by random values, the total impulse of the gas flow is *a priori* not preserved in an explicit approach. Hence, here, more realistic modelings of the

turbulent coupled two-phase fluid flow would be necessary. However, this is beyond the scope of this paper.

Here, and in the following, we want to concentrate on the modeling of the effect of the small eddies. At a "microscopic" scale, where we assume small values of the turbulent correlation time of the eddies, the effect of the small eddies on the droplets is comparable to grazing collisions. Here, following [2], we assume homogeneous isotropic turbulence in the gas phase, characterized by the microscopic specific turbulent energy $\mathscr{K}$ and the correlation time t_d. Assuming that t_d is small in comparison with the characteristic time scales of the flow, it is proved in [9, 10, 2] that the spray equation (2.2) may be replaced by the following:

$$\partial_t f + \nabla_{\mathbf{x}} \cdot (f\mathbf{v}) + \nabla_{\mathbf{v}} \cdot (f\beta) + \partial_r(f\mathscr{R}) - \nabla_{\mathbf{v}} \cdot (D\nabla_{\mathbf{v}} f) = 0. \tag{2.9}$$

Here, the expression of the diffusion coefficient is obtained by studying the dispersion in an homogeneous gas flow of a cloud of particles from a statistical point of view. Moreover, one obtains exactly the Fokker–Planck equation above in the limit where t_d is small compared to the characteristic time scales of the flow, in particular in the limit where t_d is small compared to the characteristic time scale $1/c(r)$ of the motion of a droplet in the mean gas flow (i.e., $c(r)t_d \ll 1$). When the latter condition is not satisfied, one should consider more general diffusion terms that involve more derivatives of f (see [2, 10]). However, we neglect these correction terms in this study and model the dispersed phase by using the Fokker–Planck equation (2.9) above whatever the value of $c(r)t_d$ (see also Remark **3.10** of Section **3**) . Finally, following [2], the diffusion coefficient is written

$$D \equiv D(r, \mathscr{K}, t_d) = \frac{2}{d}\frac{\mathscr{K}}{t_d}[e^{-c(r)t_d} - 1 + c(r)t_d], \tag{2.10}$$

where d is the dimension of the physical space. Note that when $c(r)t_d \gg 1$ (i.e., r tends to 0), we have $D \simeq 2c(r).\mathscr{K}/d$, whereas when $c(r)t_d \ll 1$ we have $D \simeq c^2(r).\mathscr{K}t_d/d$.

The gas phase equations should also be modified: first, we have to include a turbulence model that allows one to estimate the macroscopic and microscopic specific turbulent energies and correlation times. Obviously the effect of the droplets should also be taken into account and much effort should be geared to the derivation of two-phase turbulence models in the future. However, this is beyond the scope of this study. For the numerical experiment we use *ad hoc* laws.

Next the production terms in the right hand side of the Navier–Stokes equations should be modified since the spray equation itself was modified: straightforward computation shows that the right hand side of Eq. (2.4) is now the following:

$$\begin{cases} \mathbf{M}(\mathbf{x}, t) = \displaystyle\int_r 2K\pi\rho_l r\, dr \int_{\mathbf{v}} f\, d\mathbf{v} \\ \mathbf{I}(\mathbf{x}, t) = \displaystyle\int_r 2K\pi\rho_l r\, dr \int_{\mathbf{v}} f\mathbf{v}\, d\mathbf{v} \\ \qquad\qquad - \displaystyle\int_r c(r)\frac{4}{3}\pi\rho_l r^3\, dr \int_{\mathbf{v}} f(\mathbf{u}_g - \mathbf{v})\, d\mathbf{v} \\ \mathbf{E}(\mathbf{x}, t) = \displaystyle\int_r 2K\pi\rho_l r\, dr \int_{\mathbf{v}} f\frac{\mathbf{v}^2}{2} d\mathbf{v} \\ \qquad\qquad - 2\displaystyle\int_r c(r)\frac{4}{3}\pi\rho_l r^3\, dr \int_{\mathbf{v}} f(\mathbf{u}_g - \mathbf{v})\cdot\mathbf{v}\, d\mathbf{v} \\ \qquad\qquad - d\displaystyle\int_r D(r)\frac{4}{3}\pi\rho_l r^3\, dr \int_{\mathbf{v}} f\, d\mathbf{v}. \end{cases} \tag{2.11}$$

Remark 2.1. The equation (2.11) gives explicitly the expression of the exchange terms between the two phases so that a complete description of the two-phase fluid flow model is available. However, for the numerical implementation of the model we only need Eq. (2.6), which defines the exchange terms.

2.3. *The Semi-fluid Model*

This subsection is devoted to the derivation of the semi-fluid model. For this purpose, we must study the velocity distribution function of droplets located in a small region of the physical space. More precisely we prove the following

PROPOSITION 2.2. *Let f^0 be Gaussian in (x, v). Let f denote the solution of the* uncoupled *spray equation* (2.9) *with initial data f^0, where we consider that the gas flow data are uniform. Then, for any fixed $t \geq 0$ and for any fixed* **x** *and r, the function $\mathbf{v} \to f(\mathbf{x}, \mathbf{v}, r, t)$ is a Gaussian function.*

Proof of Proposition 2.2. We first prove the following preliminary result.

PROPOSITION 2.3. *Let f^0 be given. Let uniform gas data be given. Then the solution f of the Fokker–Planck equation* (2.9), *with initial datum f^0 may be written*

$$f(\mathbf{x}, \mathbf{v}, r, t) = S_t f^0 = \frac{1}{|J_r(t)|} \int_{\mathbf{x}'}\int_{\mathbf{v}'} \mathscr{G}_{R^-}(\mathbf{X}^- - \mathbf{x}', \mathbf{V}^- - \mathbf{v}', t) f^0(\mathbf{x}', \mathbf{v}', R^-)\, d\mathbf{x}'\, d\mathbf{v}' \tag{2.12}$$

where $(\mathbf{X}^-, \mathbf{V}^-, R^-)$ are the characteristics of Definition **3.5**

and Lemma **3.6** *below. The factor* $1/|J_r(t)|$ *is the Jacobian* $\partial(\mathbf{X}^-, \mathbf{V}^-, R^-)(t)/\partial(\mathbf{x}, \mathbf{v}, r)$ *and we have*

$$\mathcal{G}_r(\mathbf{x}, \mathbf{v}, t) = \frac{1}{(2\pi)^d \Delta_r^{d/2}(t)} \exp(-(a_r(t)\mathbf{x}^2 + 2h_r(t)\mathbf{x}\cdot\mathbf{v} + b_r(t)\mathbf{v}^2)/2\Delta_r(t)),$$

where the expressions of $a_r(t)$, $b_r(t)$, $h_r(t)$ *and* $\Delta_r(t)$ *are given in Eq.* (A.2) *of Appendix* **A**.

Proof of 2.3. The proof is given in Appendix **A**. ▌

Let us return to the proof of Proposition **2.2**. As stated in Property **3.7** below, the characteristics $(\mathbf{X}^-, \mathbf{V}^-)$ are linear functions of $(\mathbf{x}, \mathbf{v})$. Hence, if f^0 satisfies the assumptions of Proposition **2.2**, then, according to Eq. (2.12), for any fixed $t \geq 0$ and for any fixed $\mathbf{x}$ and r, the function $\mathbf{v} \to f(\mathbf{x}, \mathbf{v}, r, t)$ may be written in terms of the convolution with respect to $\mathbf{v}$ of two Gaussian functions of the variable $\mathbf{v}$ and is thus a Gaussian function of the variable $\mathbf{v}$. This concludes the proof of Proposition **2.2**. ▌

Now, in view of Proposition **2.2**, we make the following assumption for the *coupled* two-phase fluid flow system:

Hypothesis 2.4 (Modeling hypothesis). Consider the solution f of Eq. (2.9) coupled to the gas flow Eqs. (2.4) with initial datum f^0. We assume that at any point $(\mathbf{x}, r)$ and time t, the velocity distribution $\mathbf{v} \to f(\mathbf{x}, \mathbf{v}, r, t)$ is Gaussian.

Note that this hypothesis is stronger than the result of Proposition 2.2. Indeed, in Proposition 2.2, where the gas flow data are given, the mean velocity and kinetic energy of the droplets are imposed by the gas data so that here the spray may be described by only one unknown, the density. However, in the case of the kinetic modeling of the coupled system, new degrees of freedom are obtained thanks to the existence of the three exchange terms. Hence, one may introduce three unknowns for the spray independently from the unknowns of the gas flow. This is the reason why, in Hypothesis 2.4, we assume as in Proposition 2.2 that the velocity distributions of the droplets are Gaussian, but without any restriction on the possible mean velocities and variances of these distributions. Consequently, it is a stronger assumption than the result of Proposition 2.2 since we postulate here the shape of the velocity distributions for the *coupled* sytem. A mathematical study, involving appropriate scalings for the coupled problem, would be necessary to justify on rigorous grounds this modeling hypothesis, that is, to prove that Gaussian velocity distributions are relevant for the description of the spray by the semi-fluid model in the case of the coupled problem.

Thus, this hypothesis is essential from the mathematical viewpoint since it allows the derivation of the semi-fluid model below for the system, which is done here in the case where the small scale turbulent flow field is isotropic. In applications where the turbulent gas flow field is far from isotropic, more sophisticated semi-fluid models should be considered. One will finally observe that in the case of a monodisperse spray, an Eulerian description of the two-phase flow is recovered.

Remark 2.5. The assumption **2.4** does not mean that we restrict ourselves to the modeling of two-phase fluid flows such that the velocity profile of the spray, taken for instance in a section normal to the flow direction, is a Gaussian function. Such velocity distributions may be observed when sedimentation of solid particles in gas or water is studied. We expect, however, very different velocity distributions for the dispersed phase even for simple flows such as two-phase Poiseuille flow. Hypothesis **2.4** should be understood at a scale that is much smaller than the characteristic length scale. We believe that this assumption is analogous to the one which allows the Euler system of gas dynamics for large Knudsen numbers to be derived from the Boltzmann equation: for large Knudsen numbers, the velocity distribution function of the gas molecules is very close to a Gaussian function but this does not mean that the macroscopic velocity profiles are Gaussian.

Now, coming back to the modeling hypothesis, one observes that a Gaussian function is uniquely determined by its first three moments: indeed, if $\mathbf{v} \to \Xi(\mathbf{v})$ denotes a Gaussian function, Ξ is uniquely determined by the following three quantities:

$$g = \int_{\mathbf{v}} \Xi(\mathbf{v})\, d\mathbf{v}, \quad g\mathbf{u} = \int_{\mathbf{v}} \Xi(\mathbf{v})\mathbf{v}\, d\mathbf{v}, \quad ge = \int_{\mathbf{v}} \Xi(\mathbf{v}) \frac{\mathbf{v}^2}{2}\, d\mathbf{v}.$$

Then, if $d = 1, 2, 3$ is the dimension of the physical space, Ξ is written in terms of g, $\mathbf{u}$, and e as follows:

$$\Xi(\mathbf{v}) \equiv \Xi(\mathbf{v}; g, \mathbf{u}, e) = \frac{g}{[(4/d)\pi(e - \mathbf{u}^2/2)]^{d/2}} \exp\left(-\frac{(\mathbf{v}-\mathbf{u})^2}{(4/d)(e-\mathbf{u}^2/2)}\right). \tag{2.13}$$

Under Hypothesis **2.4**, the function f is thus characterized by the following three moments:

$$\begin{bmatrix} g \\ g\mathbf{u} \\ ge \end{bmatrix}(\mathbf{x}, r, t) = \begin{bmatrix} \frac{4}{3}\pi\rho_l r^3 \int_{\mathbf{v}} f(\mathbf{x}, \mathbf{v}, r, t)\, d\mathbf{v} \\ \frac{4}{3}\pi\rho_l r^3 \int_{\mathbf{v}} f(\mathbf{x}, \mathbf{v}, r, t)\mathbf{v}\, d\mathbf{v} \\ \frac{4}{3}\pi\rho_l r^3 \int_{\mathbf{v}} f(\mathbf{x}, \mathbf{v}, r, t) \frac{\mathbf{v}^2}{2}\, d\mathbf{v} \end{bmatrix}. \tag{2.14}$$

Here, due to the factor $\frac{4}{3}\pi\rho_l r^3$ in the above expression, the quantities $(g, g\mathbf{u}, ge)$ are the mass, impulse, and energy densities of the spray at the point $(\mathbf{x}, r, t)$. Note that e accounts for the kinetic energy and for the turbulent kinetic energy of the spray but is independent of the temperature of the liquid phase. To take into account the droplets' temperature would require one to introduce another dimension in the phase space.

We may now derive the semi-fluid model that characterizes the evolution of the quantities g, $g\mathbf{u}$, and ge by integrating with respect to $\mathbf{v}$ the spray equation (2.9) against the three quantities $\frac{4}{3}\pi\rho_l r^3$, $\frac{4}{3}\pi\rho_l r^3\mathbf{v}$, and $\frac{4}{3}\pi\rho_l r^3\mathbf{v}^2/2$. A straightforward computation gives the following result:

LEMMA 2.6 (Semi-fluid Model). *Consider the unknowns* $(\rho_g, \rho_g\mathbf{u}_g, \rho_g e_g)$ *for the gas and the unknown* f *for the spray solutions of the coupled equations* (2.4)–(2.9). *Assume moreover that Hypothesis* **2.4** *holds. Then the new unknowns for the spray* $(g, \mathbf{u}, e)(\mathbf{x}, r, t)$, *defined by* (2.14), *satisfy the following system of equations:*

$$\begin{cases} \partial_t g + \nabla_{\mathbf{x}} \cdot (g\mathbf{u}) - \partial_r\left(\dfrac{K}{2r} g\right) = -\dfrac{3K}{2r^2} g \\ \partial_t(g\mathbf{u}) + \nabla_{\mathbf{x}} \cdot (g\mathbf{u} \otimes \mathbf{u}) + \nabla_{\mathbf{x}} q - \partial_r\left(\dfrac{K}{2r} g\mathbf{u}\right) \\ \qquad = -\dfrac{3K}{2r^2} g\mathbf{u} - cg(\mathbf{u} - \mathbf{u}_g) \\ \partial_t(ge) + \nabla_{\mathbf{x}} \cdot (ge\mathbf{u} + q\mathbf{u}) - \partial_r\left(\dfrac{K}{2r} ge\right) \\ \qquad = -\dfrac{3K}{2r^2} ge - 2cg\left(e - \dfrac{\mathbf{u} \cdot \mathbf{u}_g}{2} - d\,\dfrac{D}{2c}\right). \end{cases} \tag{2.15}$$

Here, d *is the dimension of the physical space and* q *is the pressure-like term defined by*

$$q(\mathbf{x}, r, t) = \frac{d}{2} g\left(e - \frac{\mathbf{u}^2}{2}\right). \tag{2.16}$$

Note that if we integrate the right hand side of (2.15) with respect to the variable r, we find the opposite of the exchange terms $(\mathbf{M}, \mathbf{I}, \mathbf{E})$ defined in Eq. (2.7). That is, the exchange terms may be written explicitly in terms of the semi-fluid unknowns defined in (2.14). System (2.15) may thus be viewed as a description of the dispersed phase intermediate between a fluid model, where the unknowns would depend only on $(\mathbf{x}, t)$ and the kinetic representation by the pdf f. This is why we call it a *semi-fluid* model.

Consider now a general spray whose density function is f. *A priori,* the function f does not satisfy Hypothesis **2.4** and we may not use directly the semi-fluid model derived above. However, we shall use the following procedure which allows the use of the semi-fluid model together with the discretization of the spray unknowns: given an initial probability density function f^0, we shall approximate f^0 by a sum of functions f_k, $1 \le k \le N$, such that for each k, each $\mathbf{x}$, and each r, the function $\mathbf{v} \to f_k^0(\mathbf{x}, \mathbf{v}, r)$ is Gaussian. The probability density function f, solution of the spray equation (2.9) with initial datum f^0, is then approximated by the sum $f \simeq \sum_{k=1}^N f_k$ where, for $1 \le k \le N$, the function f_k is the solution of (2.9), with initial datum f_k^0. For each function f_k we may define the quantities g_k, $\mathbf{u}_k$, and e_k which each satisfy the semi-fluid model equation (2.15).

Finally, the problem consists in computing the unknowns $(\rho_g, \mathbf{u}_g, e_g)(\mathbf{x}, t)$, solutions of Eqs. (2.4), (2.5), and $(g_p, \mathbf{u}_p, e_p)(\mathbf{x}, r, t) = \sum_{k=1}^N (g_k, \mathbf{u}_k, e_k)(\mathbf{x}, r, t)$, where each unknown $(g_k, \mathbf{u}_k, e_k)$ is a solution of the *semi-fluid* system (2.15), (2.16). Moreover, the exchange terms (2.7) are rewritten in terms of $(g_k, \mathbf{u}_k, e_k)$. The initial data are $(\rho_g^0, \mathbf{u}_g^0, e_g^0)(\mathbf{x})$ and $(g_k^0, \mathbf{u}_k^0, e_k^0)(\mathbf{x}, r)$.

As far as we know, such a semi-fluid model does not exist in the literature. However, there already exist some methods intermediate between a fully kinetic and an Eulerian approach. For example, in the case of a polydisperse spray, one can describe the dispersed phase thanks to a set of Eulerian equations where each equation accounts for particles of a given size. Our approach is different. Here, we do not try to generalize the usual Eulerian modeling of the two-phase flows to the case of polydisperse phase. On the contrary, we are interested in a way of deriving a semi-fluid model from the most general fully kinetic model.

In the following two sections, we successively write the numerical scheme for the spray and for the gas. Moreover, we shall see that the numerical scheme for the spray introduced in the following section may be regarded either as a numerical scheme for the kinetic equation (2.9) or a numerical scheme for the semi-fluid equation (2.15) for the spray provided we assume that this description is close to the kinetic one (see the remark above). Here, the mathematical considerations of Proposition **2.2** allow us to choose a discretization of the spray consistent with the fact that we want to take into account the diffusion term in the kinetic equation (2.9).

3. A KINETIC SCHEME FOR THE SPRAY

Let Δt denote the time-step and let $t^n = n\,\Delta t$ denote the time levels. During this section we assume that the gas flow is given and constant in each cell on the interval of time $[t^n, t^{n+1}]$. The mass density field, velocity, and specific total energy field of the gas phase are respectively denoted by ρ_g^n, $\mathbf{u}_g^n$, and e_g^n.

Let us now consider the spray. We denote the initial probability density function by f^0 and, for computational purposes, we wish to approximate f^0 by Gaussian velocity

distribution functions. We may use different methods to perform this approximation. First, the finite volume method consists in defining a grid on the reduced phase space $\Omega \times (\mathbb{R}_r)_+$ and, for each cell of the grid, to approximate the restriction of f_0 to the cell by a Gaussian velocity distribution function. The parameters that characterize the Gaussian function are constant in each cell. This method allows the velocity distribution to vary as a function of the position $\mathbf{x}$ in the physical space or of the radius of the particles. Nevertheless, the reduced phase space $\Omega \times (\mathbb{R}_r)_+$ has dimension 4 and the finite volume approach is very expensive and requires many degrees of freedom. (Note that if we take into account the temperature of the droplets in the kinetic model, the dimension of the reduced phase space becomes 5 so that this dimension is always at least equal to 4.) A more efficient method by which to approximate real-valued functions defined on spaces with dimension greater or equal to 4 is the particle approximation. Here the initial datum f_0 is decomposed into the sum of a finite number of functions with a simple shape, the so-called numerical particles. Many numerical particles may be considered. It turns out, however, that in the case of our model, the most convenient numerical particles have the form

$$f_k(\mathbf{x}, \mathbf{v}, r) = \frac{1}{\frac{4}{3}\pi\rho_l r_k^3}\, \xi(\mathbf{x}; \mathbf{x}_k, m_k)\Xi(\mathbf{v}; G_k, \mathbf{U}_k, E_k) \otimes \delta(r - r_k), \tag{3.1}$$

where we omit the time-dependence and where $\mathbf{v} \to \Xi(\mathbf{v}; G_k, \mathbf{U}_k, E_k)$ is the Gaussian function whose first three moments with respect to $\mathbf{v}$ are respectively G_k, $G_k\mathbf{U}_k$, and $G_k 2E_k$ and where $\mathbf{x} \to \xi(\mathbf{x}; \mathbf{x}_k, m_k)$ is a Gaussian function, centered in $\mathbf{x}_k$, such that $m_k = \int_{\mathbf{x}} \xi(\mathbf{x}, \mathbf{x}_k, m_k)\mathbf{x}^2\, d\mathbf{x}$, and with mass unity. The numerical particles thus occupy positions around $\mathbf{x}_k$ within a range of typical size $S_k = \sqrt{m_k - (\mathbf{x}_k)^2}$. Since in our numerical method a numerical particle represents a group of particles and since the flow is turbulent, the size of a numerical particle cannot be constant and it is necessary to introduce the variable S_k, or equivalently m_k (see also Remark **3.2** below). Moreover, this variable is used in the coupling of the two phases in the numerical method since one must know here the position of the physical particles (see Section **4.2**). Finally, δ denotes Dirac's delta function. Note that the use of a Gaussian velocity distibution function is guided by the asymptotic behavior of the solutions of the spray equation (2.9), while the choice of a Gaussian function for the $\mathbf{x}$ distribution of the numerical particle is important for computational purposes.

Here $f = \sum_k^N f_k$ thus represents the state of the spray. However, thanks to the modeling hypothesis **2.4**, the spray is equivalently defined by the moments

$$(g_k, g_k\mathbf{u}_k, g_k e_k)(\mathbf{x}, r) = (G_k, G_k\mathbf{U}_k, G_k E_k)\xi(\mathbf{x}, \mathbf{x}_k, m_k) \otimes \delta(r - r_k) \tag{3.2}$$

of each function f_k with respect to $\mathbf{v}$. Hence the state of the spray is also represented by the function

$$\begin{aligned}(g_{\mathrm{p}}, g_{\mathrm{p}}\mathbf{u}_{\mathrm{p}}, g_{\mathrm{p}}e_{\mathrm{p}})(\mathbf{x}, r) &= \sum_{k=1}^{N} (g_k, g_k\mathbf{u}_k, g_k e_k)(\mathbf{x}, r) \\ &= \sum_{k=1}^{N} (G_k, G_k\mathbf{U}_k, G_k E_k)\xi(\mathbf{x}; \mathbf{x}_k, m_k) \\ &\quad \otimes \delta(r - r_k). \end{aligned} \tag{3.3}$$

However, the numerical particle (3.1) or equivalently (3.2) is characterized by the six quantities

$$(G_k, \mathbf{U}_k, E_k, \mathbf{x}_k, m_k, r_k) \tag{3.4}$$

and we shall denote a numerical particle by this vector in the sequel. The numerical particles are indexed by $1 \le k \le N$.

Now our problem is the following: given the state of the dispersed phase at time t^n in the form of the sum of numerical particles each represented by the vector (3.4), and given the gas flow, how to define the new state of the dispersed phase, at time t^{n+1}.

Recalling that the semi-fluid system (2.15) is linear we may treat the numerical particles separately. Next, the semi-fluid model is derived from the kinetic equation (2.9) so that, inspired by the ideas of Harten, Deshpande, and Perthame (see [3–5]), we introduce the following kinetic scheme for *each* numerical particle $(G_k, \mathbf{U}_k, E_k, \mathbf{x}_k, m_k, r_k)(t)$:

DEFINITION 3.1 (A Kinetic Scheme for the Spray). Let the data of the gas flow at time t^n be given. Let $(G_k^n, \mathbf{U}_k^n, E_k^n, \mathbf{x}_k^n, m_k^n, r_k^n)$ denote a numerical particle at time t^n. Then we define the numerical particle $(G_k^{n+1}, \mathbf{U}_k^{n+1}, E_k^{n+1}, \mathbf{x}_k^{n+1}, m_k^{n+1}, r_k^{n+1})$ thanks to the following algorithm consisting of the following three steps:

(a) Set

$$f_k^n(\mathbf{x}, \mathbf{v}, r) = \frac{1}{\frac{4}{3}\pi\rho_l (r_k^n)^3}\, \xi(\mathbf{x}; \mathbf{x}_k^n, m_k^n)\Xi(\mathbf{v}; G_k^n, \mathbf{U}_k^n, \mathbf{E}_k^n) \otimes \delta(r - r_k^n),$$

where Ξ is defined in Eq. (2.13).

(b) Calculate the solution f_k of the Fokker–Planck equation (2.9) for $t \ge t^n$ with initial data as f_k^n,

$$\begin{cases} \partial_t f_k + \nabla_{\mathbf{x}} \cdot (f_k\mathbf{v}) + \nabla_{\mathbf{v}} \cdot (f_k\beta) + \partial_r(f_k\mathscr{R}) - \nabla_{\mathbf{v}} \cdot (D\nabla_{\mathbf{v}} f_k) = 0 \\ f_k(\mathbf{x}, \mathbf{v}, r, t^n) = f_k^n(\mathbf{x}, \mathbf{v}, r), \end{cases}$$

where $\beta = (v - \mathbf{u}_g(\mathbf{x}_k^n, t^n))$ and $D = D(r, \mathscr{K}(\mathbf{x}_k^n, t^n), t_d(\mathbf{x}_k^n, t^n))$.

(c) Set $(G_k^{n+1}, \mathbf{U}_k^{n+1}, 2E_k^{n+1}, \mathbf{x}_k^{n+1}, m_k^{n+1}, r_k^{n+1}) = \mathscr{M}(f_k(\Delta t))$, where $\mathscr{M}$ is a projector that preserves the first three moments as well as the center of mass, the inertial momentum, and the DeBroukier radius;[3] that is

$$\begin{pmatrix} G_k^{n+1} \\ G_k^{n+1}\mathbf{U}_k^{n+1} \\ G_k^{n+1}E_k^{n+1} \\ G_k^{n+1}\mathbf{x}_k^{n+1} \\ G_k^{n+1}m_k^{n+1} \\ G_k^{n+1}r_k^{n+1} \end{pmatrix} = \int_{\mathbf{x}}\int_{\mathbf{v}}\int_r \frac{4}{3}\pi\rho_l r^3 \begin{pmatrix} 1 \\ \mathbf{v} \\ \frac{\mathbf{v}^2}{2} \\ \mathbf{x} \\ \mathbf{x}^2 \\ r \end{pmatrix} f_k(\Delta t)\, d\mathbf{x}\, d\mathbf{v}\, dr.$$

Remark 3.2. The discretization (3.3) of $(g_p, g_p\mathbf{u}_p, g_p e_p)(\mathbf{x}, r, t)$ is similar to that used in the SPH method [11, 12]. Indeed, in the SPH method for the treatment of gas dynamics as well as in our case for the treatment of the dispersed phase, the discretization consists in dividing the system into numerical particles having a given shape. In the SPH method, a numerical particle represents a particle of fluid. In our case, it represents a group of droplets. In both cases, the numerical particles follow the characteristics, which ensures a good treatment of the convection terms. Then, in order to describe the pressure terms in the SPH method, the numerical particles interact depending on their position, size, and shape. In our case, the numerical particles (i.e., the droplets) do not interact with one another but interact with the gas flow. Hence, here, the size and shape of a numerical particle allow us to take into account the effect of the gaseous turbulence on the spray.

Remark 3.3. Note that the pdf obtained in step (a) is projected onto a Gaussian velocity distribution function, mimicking what is done in usual kinetic schemes applied to the Euler system of gas dynamics. In the gas dynamics case, relaxation to a Gaussian velocity distribution function is caused by collisions between molecules and the characteristic time of this relaxation process depends on the Knudsen number: the relaxation time is very small in the case of gases at atmospheric pressure and much smaller than the time step used for numerical calculations. The projection step is thus justified on physical grounds.

[3] The DeBroukier radius r_{DB} of the distribution $\phi(r)$ is the mean radius calculated with respect to the mass of the particles, that is:

$$r_{DB}(\phi) = \frac{\int_r \frac{4}{3}\pi r^3 \phi(r) r\, dr}{\int_r \frac{4}{3}\pi r^3 \phi(r)\, dr} = \frac{\int_r r^4 \phi(r)\, dr}{\int_r r^3 \phi(r)\, dr}.$$

In the case of a spray the relaxation to a Gaussian velocity distribution function is caused by the diffusion term $\nabla_{\mathbf{v}} \cdot (D\nabla_{\mathbf{v}} f)$ in the spray equation (2.9) and the characteristic time of this relaxation may be larger than the time step of the numerical method. However, this is not a restriction for the numerical method. Indeed one observes here that the particular shape of the position and velocity distributions used for the numerical particles has no influence on the results of the kinetic scheme (see Theorem **3.4** above) nor on the coupling between the two phases. This is due to the fact that here the particles do not interact, so that the characteristic time of relaxation of the spray towards a Gaussian distribution is only governed by the characteristic of the gas, acting as an exterior force field.

We can now write the main result of this section:

THEOREM 3.4 (Solution of the Kinetic Scheme). *Let* $\mathscr{G}(\mathbf{x}, \mathbf{v}, r, t)$ *be the elementary solution of Eq.* (2.9) *for the spray and let*

$$[\sigma_x^2, -\sigma_{xv}^2, \sigma_v^2](t; r) = \int_{\mathbf{x}}\int_{\mathbf{v}} [\mathbf{x}^2, \mathbf{x}\cdot\mathbf{v}, \mathbf{v}^2]\, \mathscr{G}(\mathbf{x}, \mathbf{v}, r, t)\, d\mathbf{x}\, d\mathbf{v}$$

be the second order moments of $\mathscr{G}$. *Then, applying the kinetic scheme to the numerical particle* $(G_k^n, G_k^n\mathbf{U}_k^n, G_k^n\mathbf{E}_k^n, \mathbf{x}_k^n, m_k^n, r_k^n)$ *at time* t^n, *we have the expression for the numerical particle at time* $t > t^n$:

$$\begin{cases} G_k(t) = G_k^n \gamma^3(t - t^n; r_k^n) \\ (G_k\mathbf{U}_k)(t) = G_k^n \gamma^3(t - t^n; r_k^n)\mathbf{V}(t; \mathbf{U}_k^n, r_k^n, t^n) \\ (G_k E_k) = G_k^n \gamma^3(t - t^n; r_k^n) \\ \qquad \times \left[\frac{\mathbf{V}^2(t; \mathbf{U}_k^n, r_k^n, t^n)}{2} + \eta_1^2(t - t^n; r_k^n) \right. \\ \qquad \left. \left(\varepsilon_k^n + \frac{\sigma_v^2(t - t^n; r_k^n)}{2}\right)\right] \\ \mathbf{x}_k(t) = \mathbf{X}(t; \mathbf{x}_k^n, \mathbf{U}_k^n, r_k^n, t^n) \\ m_k(t) = \mathbf{X}^2(t; \mathbf{x}_k^n, \mathbf{U}_k^n, r_k^n, t^n) + (S_k^n)^2 + \alpha_1^2(t - t^n; r_k^n)2\varepsilon_k^n \\ \qquad + \sigma_x^2(t - t^n; r_k^n) - 2\alpha_1(t - t^n; r_k^n)\sigma_{xv}^2(t - t^n; r_k^n) \\ \qquad + \alpha_1^2(t - t^n; r_k^n)\sigma_v^2(t - t^n, r_k^n) \\ r_k(t) = R(t; r_k^n, t^n) = \gamma(t - t^n; r_k^n) r_k^n. \end{cases} \tag{3.5}$$

Here, $(\mathbf{X}, \mathbf{V}, R)$ *are the characteristics introduced in Definition* **3.5** *below with* $\mathbf{u}_g = \mathbf{u}_g(\mathbf{x}_k^n, t^n)$. *The functions* $t \to \gamma(t - t^n; r_k^n)$, $t \to \alpha_1(t - t^n; r_k^n)$ *and* $t \to \eta_1(t - t^n; r_k^n)$ *are*

the coefficients of the characteristics defined in Eq. (3.9), *and we have*

$$\begin{aligned} \varepsilon_k^n &= E_k^n - \frac{(\mathbf{U}_k^n)^2}{2} \\ (S_k^n)^2 &= m_k^n - (\mathbf{x}_k^n)^2. \end{aligned} \tag{3.6}$$

Finally, the second order moments of $\mathscr{G}$ *are explicitly written in terms of the coefficients of* $\mathscr{G}$ (*see Eq.* (A.2) *of Appendix* **A**),

$$\begin{cases} \sigma_v^2(t-t^n; r_k^n) = da_{r_k^n}(t-t^n) \\ -\sigma_{xv}^2(t-t^n; r_k^n) = -dh_{r_k^n}(t-t^n) \\ \sigma_x^2(t-t^n; r_k^n) = db_{r_k^n}(t-t^n), \end{cases} \tag{3.7}$$

where d is the dimension of the physical space.

Note that here the function $\gamma(t - t^n, r_k^n)$ denotes the ratio between the new radius $r_k(t)$ at time t of a droplet and the initial radius r_k^n at time t^n. To prove theorem **3.4** we first define the characteristics associated with the spray equation (2.9), without the diffusion terms modeling the effects of the gas turbulence:

Definition 3.5 (Characteristics). The characteristics $(\mathbf{X}, \mathbf{V}, R)(t; \mathbf{x}, \mathbf{v}, r, s)$ are defined as the solution of the following system of ordinary differential equations:

$$\begin{cases} \dfrac{d\mathbf{X}}{dt} = \mathbf{V} \\ \dfrac{d\mathbf{V}}{dt} = -c(t)(\mathbf{V} - \mathbf{u}_g) = -\dfrac{\mathscr{C}}{R^2}(\mathbf{V} - \mathbf{u}_g) \\ \dfrac{dR}{dt} = -\dfrac{K}{2R} \end{cases} \begin{cases} \mathbf{X}(s; \mathbf{x}, \mathbf{v}, r, s) = \mathbf{x} \\ \mathbf{V}(s; \mathbf{x}, \mathbf{v}, r, s) = \mathbf{v} \\ R(s; \mathbf{x}, \mathbf{v}, r, s) = r. \end{cases} \tag{3.8}$$

Note that when $t > s$, the characteristics are the solution of a Cauchy problem with initial data, whereas when $t < s$, the characteristics are the solution of a Cauchy problem with final data. Furthermore the function $t \to (\mathbf{X}, \mathbf{V}, R)(t; \mathbf{x}, \mathbf{v}, r, 0)$ is the trajectory of a single particle, initially located at the position $(\mathbf{x}, \mathbf{v}, r)$ in the phase space. For the sake of simplicity, we denote in the sequel $(\mathbf{X}^+, \mathbf{V}^+, R^+)(t) = (\mathbf{X}, \mathbf{V}, R)(t; \mathbf{x}, \mathbf{v}, r, 0)$ the *direct* characteristics, and $(\mathbf{X}^-, \mathbf{V}^-, R^-)(t) = (\mathbf{X}, \mathbf{V}, R)(0; \mathbf{x}, \mathbf{v}, r, t)$ the *reverse* characteristics. These functions may be computed explicitly:

Lemma 3.6 (Expression of the Characteristics). *Let* $\mathbf{u}_g$, *a constant, be given. The characteristics, solution of the system of ODEs* (3.8), *are written*

$$\begin{cases} \mathbf{X}(t; \mathbf{x}, \mathbf{v}, r, s) = \mathbf{x} + \dfrac{r^2}{\mathscr{C}+K}(1 - \gamma^{2+2\mathscr{C}/K}(t-s; r))\mathbf{v} \\ \qquad\qquad + \dfrac{\mathscr{C}}{\mathscr{C}+K}\left[t - \dfrac{r^2}{\mathscr{C}+K}(1 - \gamma^{2+2\mathscr{C}/K}(t-s; r))\right]\mathbf{u}_g \\ \mathbf{V}(t; \mathbf{x}, \mathbf{v}, r, s) \equiv \mathbf{V}(t; \mathbf{v}, r, s) = \gamma^{2\mathscr{C}/K}(t-s; r)\mathbf{v} \\ \qquad\qquad + \dfrac{\mathscr{C}}{\mathscr{C}+K}[1 - \gamma^{2\mathscr{C}/K}(t-s; r)]\,\mathbf{u}_g \\ R(t; \mathbf{x}, \mathbf{v}, r, s) \equiv R(t; r, s) = \sqrt{(r^2 - K(t-s))^+} = \gamma(t-s; r)r, \end{cases}$$

where we have $x^+ = \max(x, 0)$ *and* $\gamma(t - s; r) = R(t; r, s)/r$.

Proof. It suffices to integrate successively R, $\mathbf{V}$, and $\mathbf{X}$ in the ODE (3.8). Each integration involves only one unknown. ∎

We shall write in the sequel the following expressions of the three functions $\mathbf{X}$, $\mathbf{V}$, and R,

$$\begin{cases} \mathbf{X}(t; \mathbf{x}, \mathbf{v}, r, s) = \mathbf{x} + \alpha_1(t-s; r)\mathbf{v} + \alpha_2(t-s; r) \\ \mathbf{V}(t; \mathbf{v}, r, s) = \eta_1(t-s; r)\mathbf{v} + \eta_2(t-s; r) \\ R(t; r, s) = \gamma(t-s; r)r, \end{cases} \tag{3.9}$$

with obvious notations for α_i, η_i, and γ. One must remark here:

Property 3.7. The characteristics $(\mathbf{X}, \mathbf{V})(t; \mathbf{x}, \mathbf{v}, r, s)$ are linear functions of the initial position $(\mathbf{x}, \mathbf{v})$.

Let now $\mathbf{M}(\mathbf{x}, \mathbf{v}, r)$ and $f(\mathbf{x}, \mathbf{v}, r, t)$ be any functions and define the moments of f against $\mathbf{M}$ at time t as $\mathscr{M}f(t) = \int_{\mathbf{x}}\int_{\mathbf{v}}\int_r \mathbf{M} f\, d\mathbf{x}\, d\mathbf{v}\, dr$. When $f = S_t f_0$ is the solution of the kinetic equation (2.9) with initial datum f_0, a simple corollary of Proposition **2.3** is the following:

Corollary 3.8 (Moments). *Given a function* $(\mathbf{x}, \mathbf{v}, r) \to \mathbf{M}(\mathbf{x}, \mathbf{v}, r)$, *the moments at time t of* $S_t f_0$ *against* $\mathbf{M}$ *may be written as follows*:

$$\begin{aligned} (\mathscr{M}S_t f_0)(t) = \int_{\mathbf{x}'}\int_{\mathbf{v}'} d\mathbf{x}'\, d\mathbf{v}' \int_{\mathbf{x}}\int_{\mathbf{v}}\int_r f_0(\mathbf{x}', \mathbf{v}', r)\, \mathscr{G}_r(\mathbf{x}, \mathbf{v}, t) \\ \times \mathbf{M}(\mathbf{X}(t; \mathbf{x} + \mathbf{x}', \mathbf{v} + \mathbf{v}', r, 0), \\ \mathbf{V}(t; \mathbf{v} + \mathbf{v}', r, 0), R(t; r, 0))\, d\mathbf{x}\, d\mathbf{v}\, dr. \end{aligned} \tag{3.10}$$

We are now ready to prove Theorem **3.4**:

Proof of Theorem 3.4 (Solution of the Kinetic Scheme). Consider the following numerical particle:

$$f_k^n(\mathbf{x}, \mathbf{v}, r) = \frac{1}{\frac{4}{3}\pi\rho_1(r_k^n)^3}\, \xi(\mathbf{x}; \mathbf{x}_k^n, m_k^n)\Xi(\mathbf{v}; \mathbf{G}_k^n, \mathbf{U}_k^n, E_k^n) \otimes \delta(r - r_k^n). \tag{3.11}$$

Then define $\mathbf{M} = (M_j)_{j=1,5} \in \mathbb{R}^5$ as the vector $\mathbf{M} = \frac{4}{3}\pi\rho_l r^3(1, \mathbf{v}, \mathbf{v}^2/2, \mathbf{x}, \mathbf{x}^2, r)$ and let $\mathscr{M}$ denote the operator defined in Eq. (3.10). From the Definition **3.1** of the kinetic scheme, it is now clear that the kinetic scheme for the spray is written in terms of S_t and $\mathscr{M}$ as

$$(G_k^{n+1}, G_k^{n+1}\mathbf{U}_k^{n+1}, G_k^{n+1}E_k^{n+1}, G_k^{n+1}\mathbf{x}_k^{n+1}, G_k^{n+1}m_k^{n+1}, G_k^{n+1}r_k^{n+1}) = \mathscr{M}S_{\Delta t}f_k^n$$

and we know, thanks to Corollary **3.8** and the expression (3.11) of f_k^n, that we have

$$\begin{aligned}\mathscr{M}S_{\Delta t}f_k^n = {} & \frac{1}{\frac{4}{3}\pi\rho_l(r_k^n)^3} \\ & \times \int_{\mathbf{v}'}\int_{\mathbf{x}'} \xi(\mathbf{x}'; \mathbf{x}_k^n, m_k^n)\Xi(\mathbf{v}'; G_k^n, \mathbf{U}_k^n, E_k^n)\, d\mathbf{x}'\, d\mathbf{v}' \\ & \times \int_{\mathbf{x}}\int_{\mathbf{v}} \mathscr{G}_{r_k^n}(\mathbf{x}, \mathbf{v}, \Delta t) \\ & \times \mathbf{M}(\mathbf{X}(t^{n+1}; \mathbf{x}+\mathbf{x}', \mathbf{v}+\mathbf{v}', r_k^n, t^n), \\ & \quad \mathbf{V}(t^{n+1}; \mathbf{v}+\mathbf{v}', r_k^n, t^n), R(t^{n+1}; r_k^n, t^n))\, d\mathbf{x}\, d\mathbf{v}.\end{aligned}$$

We have thus to compute five moments to get the expression in Theorem **3.4**. We compute only the expression of the fifth moment $(G_k^{n+1}m_k^{n+1})$, corresponding to $M_5(\mathbf{x}, \mathbf{v}, r) = \frac{4}{3}\pi\rho_l r^3\mathbf{x}^2$, the computation of the four other moments being analogous:

$$\begin{aligned}(G_k^{n+1}m_k^{n+1}) = {} & \left(\frac{R(t^{n+1}; r_k^n, t^n)}{r_k^n}\right)^3 \\ & \times \int_{\mathbf{x}'}\int_{\mathbf{v}'} \xi(\mathbf{x}'; \mathbf{x}_k^n, m_k^n)\Xi(\mathbf{v}'; G_k^n, \mathbf{U}_k^n, E_k^n)\, d\mathbf{x}'\, d\mathbf{v}' \\ & \times \int_{\mathbf{x}}\int_{\mathbf{v}} \mathscr{G}_{r_k^n}(\mathbf{x}, \mathbf{v}, \Delta t)\mathbf{X}^2(t^{n+1}; \mathbf{x}+\mathbf{x}', \\ & \quad \mathbf{v}+\mathbf{v}', r_k^n, t^n)\, d\mathbf{x}\, d\mathbf{v}.\end{aligned} \tag{3.12}$$

Following Eq. (3.9), we shall write $\gamma(t^n - t^n; r_k^n) = R(t^{n+1}; r_k^n, t^n)/r_k^n$ from here on. Next, from Eq. (3.9), we know that the characteristic $\mathbf{X}$ writes in the form $\mathbf{X}(t; \mathbf{x}+\mathbf{x}', \mathbf{v}+\mathbf{v}', r_k^n, t^n) = \mathbf{x} + \mathbf{x}' + \alpha_1(t - t^n r_k^n)(\mathbf{v}+\mathbf{v}') + \alpha_2(t - t^n r_k^n)$, so that we may write in Eq. (3.12)

$$\begin{aligned}\mathbf{X}^2(t^{n+1}; \mathbf{x}+\mathbf{x}', \mathbf{v}+\mathbf{v}', r_k^n, t^n) & \\ = (\mathbf{x}' + \alpha_1\mathbf{v}' + \alpha_2)^2 + (\mathbf{x}^2 + 2\alpha_1\mathbf{x}\cdot\mathbf{v} + \alpha_1^2\mathbf{v}^2) & \\ + (\mathbf{x}' + \alpha_1\mathbf{v}' + \alpha_2)(\mathbf{x} + \alpha_1\mathbf{v}). &\end{aligned} \tag{3.13}$$

Then we integrate the last expression against $\int_{\mathbf{x}}\int_{\mathbf{v}} \mathscr{G}_{r_k^n}\, d\mathbf{x}\, d\mathbf{v}$. First, the contribution of the last term is zero since the function $(\mathbf{x}, \mathbf{v}) \to \mathscr{G}_{r_k^n}(\mathbf{x}, \mathbf{v})$ is centered in $\mathbf{x}$ and $\mathbf{v}$. The contribution of the second term is written exactly in terms of the second moments of $\mathscr{G}$: $\sigma_x^2 - 2\alpha_1\sigma_{xv}^2 + \alpha_1^2\sigma_v^2$. Because $\mathscr{G}$ is Gaussian in $(\mathbf{x}, \mathbf{v})$, straightforward calculations allow us to rewrite the second moments of $\mathscr{G}$ as stated in (3.7). Finally, the contribution of the first term of (3.13) in the second integral is the first term itself since $\mathscr{G}$ has mass unity. Then, rewrite the first term of (3.13) as

$$\begin{aligned}(\mathbf{x}' + \alpha_1\mathbf{v}' + \alpha_2)^2 & \\ = (\mathbf{x}_k^n + \alpha_1\mathbf{U}_k^n + \alpha_2)^2 + [(\mathbf{x}' - \mathbf{x}_k^n)^2 + \alpha_1^2(\mathbf{v}' - \mathbf{U}_k^n)^2] & \\ + 2\alpha_1(\mathbf{x}' - \mathbf{x}_k^n)(\mathbf{v}' - \mathbf{U}_k^n) & \\ + 2(\mathbf{x}_k^n + \alpha_1\mathbf{U}_k^n + \alpha_2)[(\mathbf{x}' - \mathbf{x}_k^n) + \alpha_1(\mathbf{v}' - \mathbf{U}_k^n)] &\end{aligned} \tag{3.14}$$

and calculate its contribution in Eq. (3.12). Here, we know that

$$\begin{aligned}\int_{\mathbf{x}'}\int_{\mathbf{v}'} \xi(\mathbf{x}'; \mathbf{x}_k^n, m_k^n)\Xi(\mathbf{v}'; G_k^n, \mathbf{U}_k^n, E_k^n) & \\ \left[1, \mathbf{v}', \frac{\mathbf{v}'^2}{2}, \mathbf{x}', \mathbf{x}^{2\prime}, \mathbf{x}'\cdot\mathbf{v}'\right] d\mathbf{x}\, d\mathbf{v} & \\ = [G_k^n, \mathbf{U}_k^n, E_k^n, \mathbf{x}_k^n, m_k^n, \mathbf{x}_k^n\cdot\mathbf{v}_k^n], &\end{aligned} \tag{3.15}$$

so that the contribution of the last two terms of (3.14) in Eq. (3.12) is zero. The first term is independent of $(\mathbf{x}', \mathbf{v}')$ and is exactly $\mathbf{X}^2(t^{n+1}; \mathbf{x}_k^n, \mathbf{U}_k^n, r_k^n, t^n)$, so that its contribution is $G_k^n\mathbf{X}^2(t^{n+1}; \mathbf{x}_k^n, \mathbf{U}_k^n, r_k^n, t^n)$. Finally, thanks to the definition of S_k^n and ε_k^n given in Theorem **3.4**, the contribution of the terms of Eq. (3.14) is $G_k^n(\mathbf{X}^2(t^{n+1}; \mathbf{x}_k^n, \mathbf{U}_k^n, r_k^n, t^n) + (S_k^n)^2 + \alpha_1^2 2\varepsilon_k^n)$.

Summing the contributions of (3.13) and (3.14) in (3.12) gives finally the expression of $(G_k m_k)(t)$, that is the result (3.5) stated in Theorem **3.4**. This concludes the proof of Theorem **3.4**. ▮

We have the corollary:

COLLARY 3.9. *The nonconservative unknowns* $(G_k^{n+1}, \mathbf{U}_k^{n+1}, \mathbf{x}_k^{n+1}, r_k^{n+1})$ *are the solutions at time* t^{n+1} *of the system of ODEs*

$$\begin{cases} \dfrac{dG_k}{dt} = -2\pi K r_k \\ \dfrac{d\mathbf{U}_k}{dt} = -c_k(\mathbf{U}_k - (\mathbf{u}_g)_k^n) \\ \dfrac{d\varepsilon_k}{dt} = -2c_k\left(\varepsilon_k - d\dfrac{D_k}{2c_k}\right) \\ \dfrac{d\mathbf{x}_k}{dt} = \mathbf{U}_k \\ \dfrac{dr_k}{dt} = -\dfrac{K}{2r_k} \end{cases} \quad \begin{cases} G_k(t^n) = G_k^n \\ \mathbf{U}_k(t^n) = \mathbf{U}_k^n \\ \varepsilon_k(t^n) = \varepsilon_k^n \\ \mathbf{x}_k(t^n) = \mathbf{x}_k^n \\ r_k(t^n) = r_k^n \end{cases} \tag{3.16}$$

where $c_k = c(r_k(t))$ *is the drag force coefficient defined in* (2.3) *and* $D_k = D(r_k(t), \mathscr{K}(\mathbf{x}_k^n, t^n), t_d(x_k^n, t^n))$ *is the diffusion coefficient of Eq.* (2.9) *defined in* (2.10). *Finally, the gas velocity is written here as* $(\mathbf{u}_g)_k^n = \mathbf{u}_g(\mathbf{x}_k^n, t^n)$.

Proof of Corollary 3.9. According to Theorem **3.4**, the quantities G_k^{n+1}, $\mathbf{U}_k^{n+1}$, ε_k^{n+1}, $\mathbf{x}_k^{n+1}$, and r_k^{n+1} are respectively obtained as the values of the following functions at time $t = t^{n+1}$:

$$\begin{cases} G_k(t) = \dfrac{4}{3}\pi\rho_l r_k^3(t) \\ \mathbf{U}_k(t) = \mathbf{V}(t; \mathbf{U}_k^n, r_k^n, t^n) \\ \varepsilon_k(t) = \eta_1^2(t; r_k^n, t^n)\left(\varepsilon_k^n + \dfrac{\sigma_v^2(t; r_k^n, t^n)}{2}\right) \\ \mathbf{x}_k(t) = \mathbf{X}(t; \mathbf{x}_k^n, \mathbf{U}_k^n, r_k^n, t^n) \\ r_k(t) = R(t; r_k^n, t^n). \end{cases} \tag{3.17}$$

Taking the derivatives of the above expressions with respect to t shows that the functions G_k, $\mathbf{U}_k$, $\mathbf{x}_k$, and r_k satisfy the differential equations given in Corollary **3.9**. The initial data proposed in this lemma are of course correct and the differential equations for $G_k(t)$, $\mathbf{U}_k(t)$, $\mathbf{x}_k(t)$, and $r_k(t)$ are obtained from straightforward computations. Let us now consider the kinetic energy $\varepsilon_k(t)$. We compute

$$\frac{d\varepsilon_k}{dt} = 2\frac{(d\eta_1/dt)}{\eta_1}\varepsilon_k(t) + \eta_1^2\frac{d\sigma_v^2}{dt}.$$

But we know that $\sigma_v^2(t) = da_{r_k^n}(t - t^n) = d\int_{t^n}^t D_k(s)/\eta_1^2(s)\,ds$ so that $(d\sigma_v^2/dt) = dD_k(t)/\eta_1^2(t)$. Now, from the definition of $\eta_1 = \partial_v\mathbf{V}(t; \mathbf{v})$ and the regularity of the characteristic $\mathbf{V}$ with respect to t and $\mathbf{v}$, we may write $(d\eta_1/dt) = \partial_t(\partial_v\mathbf{V}(t; \mathbf{v})) = \partial_v(\partial_t\mathbf{V}(t; \mathbf{v}))$. Thanks to Definition **3.5** of the characteristics, this gives $(d\eta_1/dt) = \partial_v[-c_k(t)(\mathbf{V}(t; \mathbf{v}) - (\mathbf{u}_g)_k^n)] = -c_k(t)\eta_1$ because c_k is independent of $\mathbf{v}$. This allows us to rewrite $d\varepsilon_k/dt$ as in Corollary **3.9**. This concludes the proof of Corollary **3.9**. ▌

Note that the expressions of the unknowns $(\mathbf{x}_k(t), \mathbf{U}_k(t), r_k(t))$ are the characteristics introduced in Definition **3.5**. This means that the position, velocity, and radius of a *numerical* particle behave like those of a *physical* particle. The same result would be obtained with more general numerical particles. Here, it suffices that the velocity distribution Ξ appearing in the kinetic scheme be a centered distribution in each direction of the velocity space. Hence, this study gives more insight on the commonly made assumption that the numerical particles follow the physical trajectories. Moreover, the equations (3.16) for $\mathbf{U}_k(t)$ and $\varepsilon_k(t)$ show that the mean velocity and the specific internal kinetic energy of the numerical particle are equivalent to $\mathbf{u}_g$ and $dD/(2c)$, respectively, when t becomes large. This result is consistent with the semi-fluid system (2.15) for the spray. Note also that when $K = 0$, the limit $dD/(2c)$ of $\varepsilon_k(t)$ as t tends to infinity is a constant. This corresponds to a ''thermalization'' of the cloud of particles.

Remark 3.10. Notice that this value $dD/(2c(r))$ is always less than the (microscopic) turbulent kinetic energy of the gas. Indeed, the diffusion term D accounts for the dispersion of particles. On the one hand, when $c(r)t_d \gg 1$, that is when the droplets may be considered as passive scalars, we then find $dD/(2c(r)) = \mathscr{K}$, that is the agitation of the particles equals that of the gas. On the other hand, when $c(r)t_d \ll 1$, we have $dD/(2c(r)) = \mathscr{K}(c(r)t_d/2)$, which means that only a fraction of the turbulent kinetic energy of the gas participates to the dispersion of the droplets.

Remark* 3.11. Theorem **3.4 and Corollary **3.9** are available in both the laminar and turbulent cases, as well as in the burning and non-burning cases. In the laminar case, the expressions are simply rewritten with $D = 0$. In the case of non-burning droplets, that is, in the limit where K tends to zero, we simply write $K = 0$, $\gamma(t; r_k^n, s) = 1$, $\eta_1(t - s; r_k^n) = e^{-c(t-s)}$, and $\alpha_1(t - s; r_k^n) = (1 - e^{-c(t-s)})/c$ in all the expressions. Hence, in the case of non-burning droplets, that is, when $K = 0$, the characteristics are simply given by the following expressions:

$$\begin{cases} \mathbf{X}(t; \mathbf{x}, \mathbf{v}, r, s) = \mathbf{x} + \dfrac{1 - e^{-c(t-s)}}{\mathbf{c}}\mathbf{v} + \left((t-s) - \dfrac{1 - e^{-c(t-s)}}{c}\right)\mathbf{u}_g \\ \mathbf{V}(t; \mathbf{v}, r, s) = e^{-c(t-s)}\mathbf{v} + (1 - e^{-c(t-s)})\mathbf{u}_g \\ R(t; r, s) = r. \end{cases} \tag{3.18}$$

4. A FINITE VOLUME SCHEME FOR THE GAS UNKNOWNS

4.1. *The Gas Scheme*

This subsection is devoted to the construction of a numerical scheme for approximating the quantities relative to the gas flow. The scheme below is written in two space dimensions but may easily be extended to the three-dimensional case. We chose a finite volume method for approximating the solution of the Navier–Stokes equations (2.4) which may be written in the following condensed form:

$$\begin{aligned} &\partial_t W + [\partial_x F(W) + \partial_y G(W)] \\ &\quad + [\partial_x P(W, \nabla W) + \partial_y Q(W, \nabla W)] = Z. \end{aligned} \tag{4.1}$$

Here, writing $\mathbf{u}_g = (u, v)$, we have

$$
\begin{aligned}
W &= (\rho, \rho u, \rho v, \rho e)^{\mathrm{T}} \\
F(W) &= (\rho u, \rho u^2 + p, \rho uv, (\rho e + p)u) \\
G(W) &= (\rho v, \rho uv, \rho v^2 + p, (\rho e + p)v) \\
P(W, \nabla W) &= (0, \mu_g 2\partial_x u + \lambda(\partial_x u + \partial_y v), \mu_g(\partial_x v + \partial_y u), \\
&\quad [\mu_g 2\partial_x u + \lambda(\partial_x u + \partial_y v)]u \\
&\quad + [\mu_g(\partial_x v + \partial_y u)]v + \kappa \partial_x \varepsilon) \\
Q(W, \nabla W) &= (0, \mu_g(\partial_x v + \partial_y u), \mu_g 2\partial_x v \\
&\quad + \lambda(\partial_x u + \partial_y v), [\mu_g(\partial_x v + \partial_y u)]u \\
&\quad + [\mu_g 2\partial_y v + \lambda(\partial_x u + \partial_y v)]v + \kappa \partial_y \varepsilon) \\
Z &= (\mathbf{M}, \mathbf{I}, \mathbf{E}).
\end{aligned}
$$

Note that the subscript g is omitted in the above expressions. The quantity p is the gas pressure, given by $p = (\gamma - 1)\rho(e - \frac{1}{2}(u^2 + v^2))$, while F and G denote the convection fluxes of Eq. (2.4) and, P and Q are the viscous fluxes.

Now, let a mesh be given whose cell are denoted by $\mathscr{C}_i$, $1 \le i \le I$. These cells are quadrangles or triangles. In the cell-center approach, one considers the quantity $W_i(t)$, defined as the mean value of W over the cell $\mathscr{C}_i$,

$$
W_i(t) = \frac{1}{|\mathscr{C}_i|} \int_{\mathscr{C}_i} W(\mathbf{x}, t)\, d\mathbf{x},
$$

where $|\mathscr{C}_i|$ denotes the surface of the cell $\mathscr{C}_i$. The numerical scheme is aimed at defining an approximation of the quantities $W_i(t^n)$, $1 \le i \le I$, $n \ge 0$. Of course the quantities $W_i(t^0)$ are given in terms of the initial data. In order to write the numerical scheme assume first that an exact smooth W of (4.1) is known. Then integrate Eq. (4.1) over $\mathscr{C}_i$,

$$
\begin{aligned}
\frac{d}{dt} W_i + \frac{1}{|\mathscr{C}_i|} \int_{\partial \mathscr{C}_i} &([F(W)n_x + G(W)n_y] \\
&+ [P(W, \nabla W)n_x + Q(W, \nabla W)n_y])\, ds = \Omega_i
\end{aligned}
\tag{4.2}
$$

where $\partial \mathscr{C}_i$ is the boundary of $\mathscr{C}_i$, $\mathbf{n} = (n_x, n_y)^{\mathrm{T}}$ is the outward unit normal to $\mathscr{C}_i$ on $\partial \mathscr{C}_i$, s is the arc-length abscissa on $\partial \mathscr{C}_i$ and where we have

$$
Z_i(t) = \frac{1}{|\mathscr{C}_i|} \int_{\mathscr{C}_i} Z(\mathbf{x}, t)\, d\mathbf{x}
$$

Considering next the cells $\mathscr{C}_j$, neighboring $\mathscr{C}_i$, Eq. (4.2) may be rewritten as follows:

$$
\frac{d}{dt} W_i + \sum_{i \ne j} \frac{1}{|\mathscr{C}_i|} \int_{\partial \mathscr{C}_i \cap \partial \mathscr{C}_j} \mathscr{F}\, ds + \sum_{i \ne j} \frac{1}{|\mathscr{C}_i|} \int_{\partial \mathscr{C}_i \cap \partial \mathscr{C}_j} \mathscr{P}\, ds = Z_i
$$

where $\mathscr{F} = [F, G]$ and $\mathscr{P} = [P, Q]$. Finally, assume that $\mathscr{F}_{ij}$ (resp. $\mathscr{P}_{ij}$) is a numerical approximation of the flux $\mathscr{F}$ (resp. $\mathscr{P}$) on the interface $\partial \mathscr{C}_i \cap \partial \mathscr{C}_j$. Let L_{ij} and $\mathbf{n}_{ij}$ be respectively the length of the interface $\partial \mathscr{C}_i \cap \partial \mathscr{C}_j$ and the outward unit normal to $\mathscr{C}_i$ on the interface. Then we write the following semi-discrete numerical scheme:

$$
\frac{d}{dt} W_i + \sum_{i \ne j} \mathscr{F}_{ij} \cdot \mathbf{n}_{ij} \frac{L_{ij}}{|\mathscr{C}_i|} + \sum_{i \ne j} \mathscr{P}_{ij} \cdot \mathbf{n}_{ij} \frac{L_{ij}}{|\mathscr{C}_i|} = Z_i.
$$

Now, let W_i^n (respectively $\mathscr{F}_{ij}^n$, $\mathscr{P}_{ij}^n$, and Z_i^n) denote the approximate value of $W_i(t^n)$ (respectively $\mathscr{F}_i(t^n)$, $\mathscr{P}_i(t^n)$, and $Z_i(t^n)$), where $t^n = n\,\Delta t$. A first order numerical scheme for the unknowns $(W_i)_{i=1,I}$ is

$$
\frac{W_i^{n+1} - W_i^n}{\Delta t} + \sum_{i \ne j} \Phi_{ij}^n \frac{L_{ij}}{|\mathscr{C}_i|} + \sum_{i \ne j} \Psi_{ij}^n \frac{L_{ij}}{|\mathscr{C}_i|} = Z_i^n, \tag{4.3}
$$

where $\Phi_{ij}^n = \mathscr{F}_{ij}^n \cdot \mathbf{n}_{ij}$ and $\Psi_{ij}^n = \mathscr{P}_{ij}(W_i^n, \nabla W_i^n) \cdot n_{ij}$. We expect this scheme to be stable under the following CFL condition (note that the diffusion terms are treated implicitly so that no stability condition is associated with these terms),

$$
\Delta t \le \Delta T_{\mathrm{CFL}} \tag{4.4}
$$

where ΔT_{CFL} will be defined later. The end of the section is devoted to the derivation of the approximate fluxes $\mathscr{F}_{ij}^n$ and $\mathscr{P}_{ij}^n$.

Consider first the convection fluxes $\Phi_{ij}^n = \mathscr{F}_{ij}^n \cdot \mathbf{n}_{ij}$. A convenient approximation of this flux is provided by the solution of a one-dimensional Riemann problem in the direction normal to the interface whose left and right states are respectively W_i^n and W_j^n (see [13]). Further, an approximate Riemann solver may be used. In other words, if $W_{ij}(t > t^n)$ is the value of the *exact solution of the Riemann problem* on the interface, we set $\mathscr{F}_{ij}^n = \mathscr{F}(W_{ij})$, which also defines Φ_{ij}^n. We call this process a *Riemann solver* and denote it in the following condensed way: $\Phi_{ij}^n = \Phi(W_i^n, \mathbf{n}_{ij}, W_j^n)$. We use the Roe solver here so that the convection terms in the scheme (4.3) are written

$$
\Phi_{ij}^n = \Phi_{\mathrm{Roe}}(W_i^n, \mathbf{n}_{ij}, W_j^n). \tag{4.5}
$$

We expect that Roe's scheme is stable under the CFL condition

$$
\sup_{i,j,p,n} \Delta T_{\mathrm{CFL}} \frac{d_i |\lambda_{ij}^{n,p}|}{|\mathscr{C}_i|} \le \frac{1}{2}, \tag{4.6}
$$

where d_i is the diameter of the greatest circle contained in $\mathscr{C}_i$ and $(\lambda_{ij}^{n,p})_{p=1,4}$ denote the eigenvalues of the Roe's matrix $\mathscr{A}_{\mathrm{Roe}}(W_i^n, \mathbf{n}_{ij}, W_j^n)$ at the interface $\partial \mathscr{C}_i \cap \partial \mathscr{C}_j$ at time

t^n. The main advantage of using Roe's numerical scheme is that it provides us with a robust and efficient scheme for the discretization of the convection terms. But Roe's method may replace some rarefaction waves by nonphysical discontinuous weak solutions of the Euler system of gas dynamics. Such spurious solutions are expected when sonic points are present in rarefaction waves. In order to avoid them, an entropy correction is needed. Here, we use Roe's entropy correction (see [14] for more details).

Consider next the second order term $\Psi_{ij}^n = \mathscr{P}_{ij}(W_i^n, \nabla W_i^n)\cdot \mathbf{n}_{ij}$ in the scheme (4.3). Omitting the superscript n, $\mathscr{P}_{ij}$ stands for an approximation of $\mathscr{P}(W, \nabla W)(\mathbf{a}_{ij})$, where $\mathbf{a}_{ij}$ denotes the center of the interface $\partial\mathscr{C}_i \cap \partial\mathscr{C}_i$, so that we may define

$$\mathscr{P}_{ij} = \mathscr{P}(W_{ij}, \nabla W_{ij}),$$

where W_{ij} and ∇W_{ij} are approximate values of $W(a_{ij})$ and $\nabla W(\mathbf{a}_{ij})$, respectively. But $\mathbf{a}_{ij}$ is the center of $\partial\mathscr{C}_i \cap \partial\mathscr{C}_j$: $a_{ij} = \frac{1}{2}(\mathbf{a}_{ij}^- + \mathbf{a}_{ij}^+)$, where $\mathbf{a}_{ij}^{\pm}$ are the vertices of the segment $\partial\mathscr{C}_i \cap \partial\mathscr{C}_j$, and we set $W_{ij} = \frac{1}{2}(W_{ij}^- + W_{ij}^+)$ (resp. $\nabla W_{ij} = \frac{1}{2}(\nabla W_{ij}^- + \nabla W_{ij}^+)$) where $W_{ij}^{\pm}$ (resp. $\nabla W_{ij}^{\pm}$) are some approximate values of $W(\mathbf{a}_{ij}^{\pm})$ (resp. $\nabla W(\mathbf{a}_{ij}^{\pm})$). Now, it is possible to define $W_{ij}^{\pm}$ and $\nabla W_{ij}^{\pm}$ in terms of the unknowns $(W_i)_{i=1,I}$. Let indeed $\mathscr{C}_m$ denote a cell for which $\mathbf{a}_{ij}^-$ is a vertex. We define the control volume $\mathscr{V}(\mathbf{a}_{ij}^-)$ around $\mathbf{a}_{ij}^-$ as the union of the cells $\mathscr{C}_m$ that contain $\mathbf{a}_{ij}^-$: $\mathscr{V}(a_{ij}^-) = \bigcup_m \mathscr{C}_m$. Then, we may define W_{ij}^- as the average

$$W_{ij}^- = \frac{1}{|\mathscr{V}(a_{ij}^-)|}\int_{\mathscr{V}(\mathbf{a}_{ij}^-)} W(\mathbf{x})\,d\mathbf{x} = \sum_m \frac{|\mathscr{C}_m|}{|\mathscr{V}(\mathbf{a}_{ij}^-)|}\,W_m.$$

The quantity W_{ij}^+ is defined in the same manner, and finally, we succeed in writing W_{ij} in terms of the unknowns $(W_i)_{i=1,I}$.

The term ∇W_{ij} is also defined as $\nabla W_{ij} = \frac{1}{2}(\nabla W_{ij}^- + \nabla W_{ij}^+)$ and the quantity ∇W_{ij}^- (resp. ∇W_{ij}^+) is approximated by the mean of the same quantity over a control volume around $\mathbf{a}_{ij}^-$ (resp. $\mathbf{a}_{ij}^+$). But here, using the Stokes formula, we write

$$\begin{aligned}\nabla W_{ij}^- &= \frac{1}{|\mathscr{V}(\mathbf{a}_{ij}^-)|}\int_{\mathscr{V}(\mathbf{a}_{ij}^-)} \nabla W(\mathbf{x})\,d\mathbf{x} = \frac{1}{|\mathscr{V}(\mathbf{a}_{ij}^-)|}\int_{\partial\mathscr{V}(\mathbf{a}_{ij}^-)} W\cdot\mathbf{n}\,ds\\ &\simeq \frac{1}{|\mathscr{V}(\mathbf{a}_{ij}^-)|}\sum_j L_{mj}W_m\cdot\mathbf{n}_{mj}\end{aligned}$$

with obvious notations. Finally, the viscous terms in the numerical scheme (4.3) are written as follows:

$$\Psi_{ij}^n = \mathscr{P}(W_{ij}^n, \nabla W_{ij}^n)\cdot\mathbf{n}_{ij}. \tag{4.7}$$

Hence, the scheme for the gas consists of Eqs. (4.3), (4.4), (4.5), (4.6), (4.6), (4.7) plus the expression (4.12) below of $Z_i^n\,\Delta t$, given in the following subsection.

4.2. *The Coupling between the Two Phases*

After the introduction of numerical schemes that compute approximate values of the quantities relative to both phases, it remains for us to explain how the source terms in the Navier–Stokes equations (2.4) and in the semi-fluid model (2.15) are treated. The method that we use is inspired by particle in cell approximations.

We first consider the approximation of the production terms in the system of the Navier–Stokes equations (2.15). Set $\mathbf{g}_k^n = (G_k^n, \mathbf{U}_k^n, E_k^n, \mathbf{x}_k^n, m_k^n, r_k^n)$, the vector that characterizes the kth numerical particle at time $t = t^n$. The source terms in cell $\mathscr{C}_i$ are given by the expression

$$Z_i\,\Delta t \overset{\text{def}}{=} \int_{t^n}^{t^{n+1}}\int_{\mathscr{C}_i} (\mathbf{M}, \mathbf{I}, \mathbf{E})(\mathbf{x}, t)\,d\mathbf{x}\,dt \tag{4.8}$$

and we want to write the last expression in term of the vectors $\mathbf{g}_k^n$, $1 \le k \le K$. According to Eq. (2.6), the quantity Z_i is given by

$$\begin{aligned}Z_i\,\Delta t = \int_{t^n}^{t^{n+1}}\int_{\mathscr{C}_i}\Bigg[\partial_t\int_{\mathbf{v}}\int_r f\phi(\mathbf{v}, r)\,d\mathbf{v}\,dr\\ + \nabla_{\mathbf{x}}\cdot\left(\int_{\mathbf{v}}\int_r f\mathbf{v}\phi(\mathbf{v}, r)\,d\mathbf{v}\,dr\right)\Bigg]\,d\mathbf{x}\,dt.\end{aligned} \tag{4.9}$$

Assume for the sake of simplicity that during the interval of time $[t^n, t^{n+1}]$ the particles either do not enter the cell $\mathscr{C}_i$, or stay in the cell $\mathscr{C}_i$. Then, the integral of the divergence term in the last expression vanishes and we may write the following expression for Z_i:

$$\begin{aligned}Z_i\,\Delta t &\overset{\text{def}}{=} \int_{t^n}^{t^{n+1}}\int_{\mathscr{C}_i} (\mathbf{M}, \mathbf{I}, \mathbf{E})(\mathbf{x}, t)\,d\mathbf{x}\,dt\\ &= -\sum_{\mathbf{x}_k(t)\in\mathscr{C}_i}([G_k^{n+1}, G_k^{n+1}\mathbf{U}_k^{n+1}, G_k^{n+1}E_k^{n+1}]\\ &\quad - [G_k^n, G_k^n\mathbf{U}_k^n, G_k^nE_k^n]).\end{aligned} \tag{4.10}$$

Next, the numerical particle $\mathbf{g}_k^n$ has a non-zero diameter and lies in the ball B_k^n with center $\mathbf{x}_k^n$ and diameter S_k^n. We have thus to consider the following events:

(i) During $[t^n, t^{n+1}]$, a numerical particle crosses more than one cell.

(ii) For some $t \in [t^n, t^{n+1}]$, $\mathbf{x}_k(t) \in \mathscr{C}_i$, but the ball B_k^n is not subset of $\mathscr{C}_i$.

The first event means that the center of a numerical particle may cross different cells during $[t^n, t^{n+1}]$, so differ-

ent values of the data of the gas flow should be considered during one time step. However, in the case of a numerical scheme of the first order in the space and time variables event (i) is not a constraint. Indeed, we expect velocities of the particles smaller than or comparable to the velocity of the waves in the gas. Hence, since the CFL condition holds for the gas unknowns, during one timestep the length of the path of a particle is less than or of order of the size of a computational cell, which may be written in terms of the CFL-like condition for the droplets,

$$\sup_{i,k_i,n} \Delta t \frac{|\mathbf{u}_{k_i}^n|}{d_i} \leq 1, \tag{4.11}$$

where d_i is the diameter of the cell $\mathscr{C}_i$. Consequently, one can compute here the motion of a given numerical particle of index k thanks to the gas variables at $(\mathbf{x}_k^n, t^n)$. In the case of a second order numerical scheme, modifications of the method are needed (see Section **4.3** below).

Now, consider the second event. When the size S_k^n of a numerical particles exceeds that of the surrounding cells, we may proceed in one of the following two manners. First, we can split the numerical particle. However, in strongly turbulent flows this first method may increase the number of numerical particles exponentially. Hence, a second manner of dealing with this event is to use a random walk: if a numerical particle has the volume S_k^n exceeding that of the surrounding cells, we proceed to a random walk of length $(S_k^n)^{1/2}$ and then set the dimension of the numerical particle to zero. This random walk is consistent with the diffusion term in the Fokker–Planck equation and may be interpreted as follows: the pdf f, solution of the Fokker–Planck equation (2.9), represents the motion of particles in a turbulent gas flow. However, the function f is a mean solution in a statistical sense. Consider a single particle in a turbulent gas flow. Its motion is a random walk. Here, the pdf f accounts for all the possible random walks of the particle. Hence, though a numerical particle may represent only a few physical particles, that is, $S_k(0) \simeq 0$ at time $t = 0$, we may have for $t > 0$, $S_k(t) > 0$, accounting for the uncertainty about the position of the droplets at $t > 0$. More details concerning the statistics of the motion of the droplets in a turbulent gas flow field are available in Ref. [2].

Finally, the exchange term in the scheme (4.3) for the gas are written as follows:

$$Z_i \Delta t = -\sum_k \frac{|B_k^n \cap \mathscr{C}_i|}{|B_k^n|} ([G_k^{n+1}, G_k^{n+1}\mathbf{U}_k^{n+1}, G_k^{n+1}E_k^{n+1}] - [G_k^n, G_k^n\mathbf{U}_k^n, G_k^nE_k^n]). \tag{4.12}$$

However, if the control volumes $\mathscr{C}_i$ are simple, rectangles, as in the example calculations below, then the intersection volumes $|B_k^n \cap \mathscr{C}_i|$ are easy to calculate. In the case where the control volumes have more complicated shapes, the calculation of the intersection volumes may become much more difficult.

Finally, considering this coupling, the scheme for the whole system is "locally" conservative on a space scale of order $\max_{k,n} S_k^n$. Nevertheless the scheme for the whole system is globally conservative, since for any $n \in \mathbb{N}$, we have

$$\sum_i (W_i^{n+1} - W_i^n) + \sum_k ([G_k^{n+1}, G_k^{n+1}\mathbf{U}_k^{n+1}, G_k^{n+1}E_k^{n+1}] - [G_k^n, G_k^n\mathbf{U}_k^n, G_k^nE_k^n]) = 0,$$

where we omit the boundary conditions.

Remark 4.1. The motion of the numerical particle located at $\mathbf{x}_i(t)$ depends on the datas of the gas flow at position $\mathbf{x}_i(t)$ and time t. Since the gas is discretized by a finite volume approach, we had to interpolate the datas of the gas flow field on the particles, then project the datas of the particles on the mesh. Similar difficulties appear in the PIC methods (see [15]).

4.3. *Extensions*

The numerical method described above extends to more general physical laws for the motion of the droplets and to the second order in time and space variables in the following manner.

For a general drag force written in the form

$$\frac{d\mathbf{v}}{dt} = -\frac{1}{t_r}(\mathbf{v} - \mathbf{u}_g), \tag{4.13}$$

where t_r is the characteristic time of the motion of a droplet of radius r in the gas and may be a complex function of all the variables of the system, we simply set in our method the drag force coefficient c at time t^n as $c = (1/t_r)(t^n)$ and compute the motion of the droplet during the timestep $[t^n, t^{n+1}]$.

We proceed in the same manner for a vaporization law written in the form

$$\frac{dr}{dt} = -\frac{K}{2r}, \tag{4.14}$$

where K is no longer a constant but any function of the variables of the system.

Now, for the extension of the method to the second order in space, we proceed in the following manner. Here, the data of the gas flow are known as polynomials of the first order in each cell. Let a numerical particle k be in the

cell $\mathscr{C}_i$ at time t^n. We interpolate at the second order the velocity $\mathbf{u}_g^n$ of the gas at the position $\mathbf{x}_k^n$ of the numerical particle and then predict the position $\tilde{\mathbf{x}}_k^{n+1}$ of the numerical particle at time t^{n+1} therefore located in the cell $\tilde{\mathscr{C}}_i$. Moreover at $\tilde{\mathbf{x}}_k^{n+1}$, the gas velocity is $\tilde{\mathbf{u}}_g^{n+1}$, the drag coefficient is $\widetilde{(1/t_r)}(t^{n+1})$ and the vaporization coefficient is $\tilde{K}(t^{n+1})$. Finally, we calculate again the motion of the numerical particle located at the initial position $\mathbf{x}_k^n$ at time t^n which "sees" the gas velocity $(\mathbf{u}_g^n + \tilde{\mathbf{u}}_g^{n+1})/2$, with drag coefficient $[(1/t_r)(t^n) + \widetilde{(1/t_r)}(t^{n+1})]/2$ and vaporization coefficient $[K(t^n) + \tilde{K}(t^{n+1})]/2$. The motion of the numerical particle is therefore computed at the second order and the exchange terms induced by the motion of the numerical particle are equally distributed to the cells $\mathscr{C}_i$ and $\tilde{\mathscr{C}}_i$. This procedure gives a second order numerical scheme in the space variable for the system.

For extension to second order in time, it suffices to use a classical operator splitting method where a timestep of size Δt consists now in the following sequence:

- During $\Delta t/2$, compute the motion of the numerical particles and exchange moments with the gas.
- During Δt, compute the motion of the gas.
- During $\Delta t/2$, compute the motion of the numerical particles and exchange moments with the gas.

5. NUMERICAL RESULTS

- We first consider the case of the injection of droplets of water into a closed chamber. In this experiment we consider the non-turbulent equation for the spray, that is, the diffusion coefficient D in Eq. (2.9) is zero. The chamber is 10 cm long and 5 cm high and contains air at the temperature $T = 300$ K, at atmospheric pressure: $p = 10^5$ Pa. We set here for the viscosity of the gas $\mu_g(\mathbf{x}) = \mu_g^0\sqrt{T(\mathbf{x})}\,\mathrm{m}^2/\mathrm{s}$, where $T(\mathbf{x})$ is the gas temperature in Kelvin and $\mu_g^0 = 1.26 \times 10^{-6}$. Then the volume is discretized with square shaped cells of size 1.25 mm.

The nonevaporating droplets are injected during the interval of time $T = 1$ ms from the left side of the chamber, in the horizontal direction. The droplets that are injected all have the same radius $r = 5\ \mu$m: we say that the spray is monodisperse. The total mass of liquid is $M_T = 5 \times 10^{-3}$ kg, and this mass is of the same order as the mass of the gas initially contained in the chamber. The droplets are injected with a velocity $V = 100$ m/s. The vertical component V_y is randomly chosen in the interval $[-8$ m/s, $+ 8$ m/s] with a uniform law. The horizontal component of the injection velocity is then $V_x = (100^2 - V_y^2)^{1/2}$. Now, let $K = 90$ be the number of numerical particles per cell near the injector. Then the interval of time between the injection of two packets of particles is $\Delta t_i = \Delta x/(KV)$, where V is the injection velocity and Δx is the width of the cells. Finally, the mass flow of the injector is $Q = M_T/T$. Hence, every Δt_i s, a numerical particle is injected with a random velocity as described before. Each numerical particle represents a group of droplets of radius r with total mass $M_p = Q\,\Delta t_i = (M_T/T)\,\Delta t_i$.

The results of the computations are shown in Fig. 1: we show the repartition of the computed mass of the droplets in the chamber every 0.1 ms between 0.1 and 1 ms.

We observe how the spray evolves and splits due to the recirculation of the gas in the chamber. Also, the diameter of the liquid jet increases with the distance from the injection point, due to the interaction between the droplets and gas. As usual when Lagrangian methods are used, the interface between the liquid jet and the region with no droplets in the chamber is easily and precisely computed.

The mean velocity field at time $t = 1$ ms is shown in Fig. 2. The maximal computed velocity is 93.2 m/s.

In this computation, taking the gas quantities as constant, we integrate exactly the trajectory of the numerical particles, thanks to formula (3.18). However, many popular methods use the following quadrature to determine the position of the numerical particles at time t^n as a function of the position in the phase space at time t^n,

$$\begin{cases} \mathbf{x}(t^{n+1}) = \mathbf{x}(t^n) + \mathbf{v}(t^n)\,\Delta t \\ \mathbf{v}(t^{n+1}) = (1 - c\,\Delta t)\mathbf{v}(t^n) + c\,\Delta t\,\mathbf{u}_g^n, \end{cases}$$

where $\Delta t = t^{n+1} - t^n$. Moreover, when $c\,\Delta t > 1$ we must impose $v(t^{n+1}) = \mathbf{u}_g^n$. This means that when the time $t_{\mathrm{drag}} = 1/c$ of capture of a droplet is larger than the timestep Δt, we impose that the velocity of the droplet equals that of the gas. In order to evaluate the differences between the two methods, we introduce the *local* relative error $|m_1 - m_2|(\mathbf{x})/\max(m_1(\mathbf{x}), m_2(\mathbf{x}))$ in each cell. Here, $m_1(\mathbf{x})$ is the mass of droplets computed with the exact expressions given in formula (3.18), $m_2(\mathbf{x})$ is the mass of droplets computed with the approximation formula above. Hence, this error is a *local* measure of the differences between the two methods and ranges in the interval [0, 1]. We plot this error in Fig. 3 below. Note that the relative error equals 1 in a given cell when one of the two methods predicts a positive mass in the cell while the other method predicts that there are no droplets in that cell. Therefore, a significant "local" relative error between the two methods does not mean a significant difference between the aspects of the two-phase flow observed in the two methods. However, roughly speaking, this "local" error measures the ratio of mass that one should displace from a given cell to a neighboring cell in order to obtain the spray observed in a first experiment when given the spray in a second experiment. Finally, we expect that the error increases when the drag coefficient c increases, that is when we consider smallest droplets. We observe here that the local relative error concentrates in the recirculation zone.

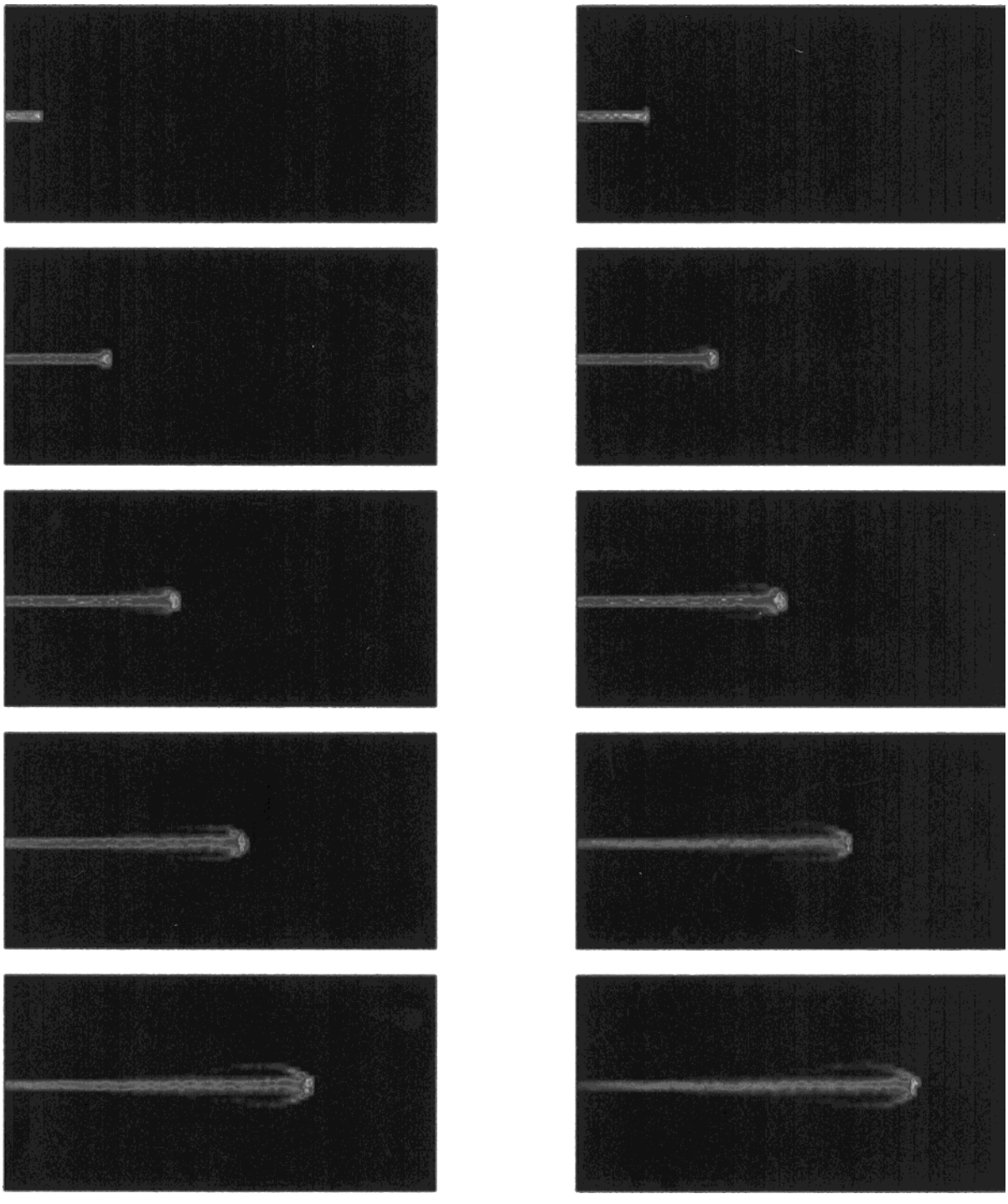

FIG. 1. First experiment: chamber without turbulence modeling. Mass of the liquid in the chamber for times 0.1 to 1 ms.

Now, we compute the *global* relative error at final time $t = 1$ ms,

$$\frac{\|m_1 - m_2\|_1}{M_T},$$

where M_T is the total mass injected. Hence, this global relative error measures the mass displaced when the spray is computed by one method or the other. This total mass equals only 1% of the total mass injected, which is not very much. We believe that the coupling with the gas stabilizes

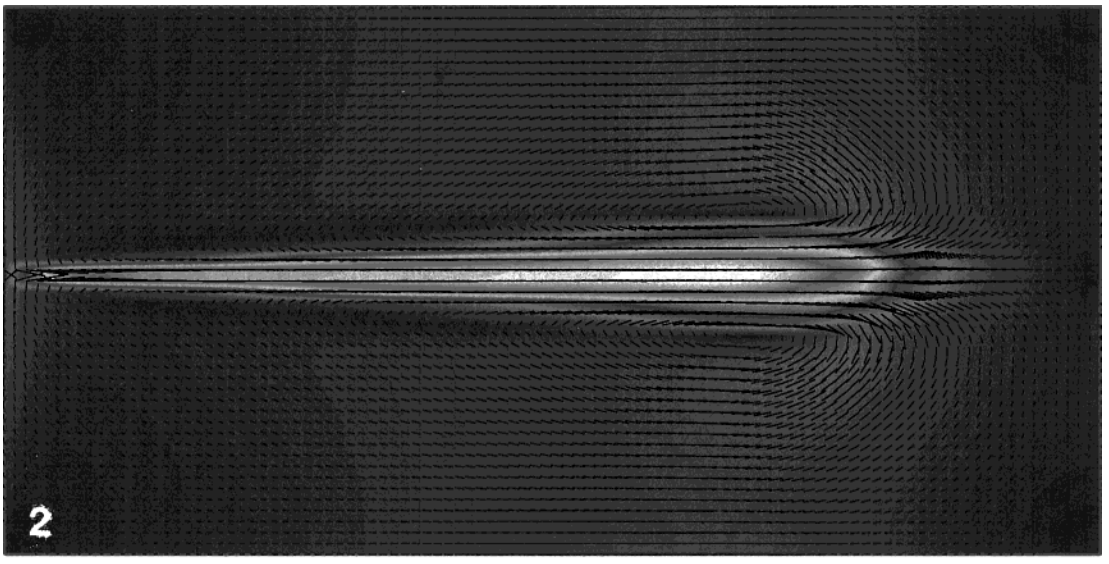
2

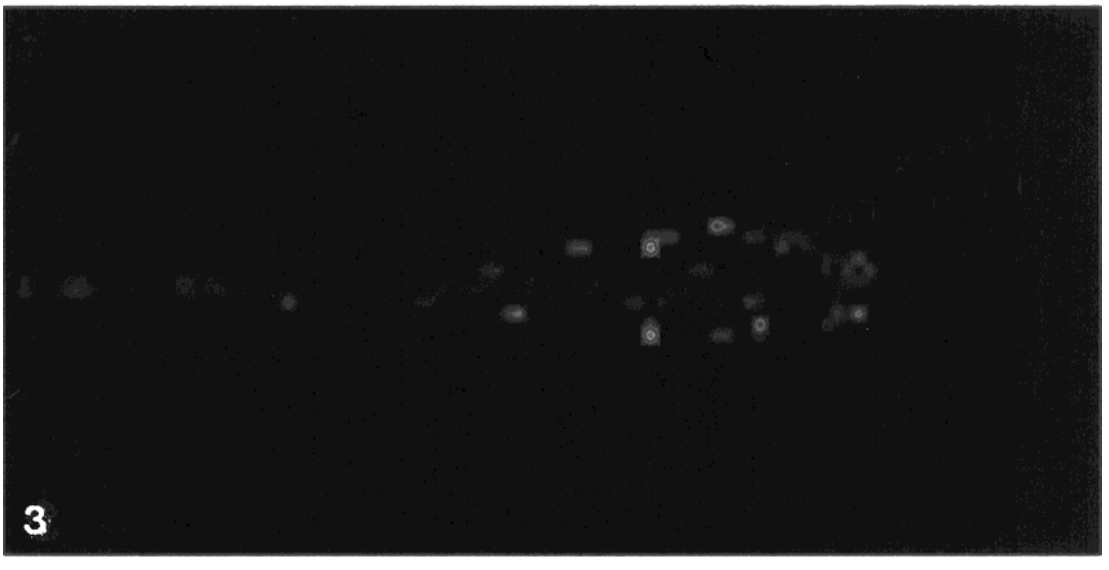
3

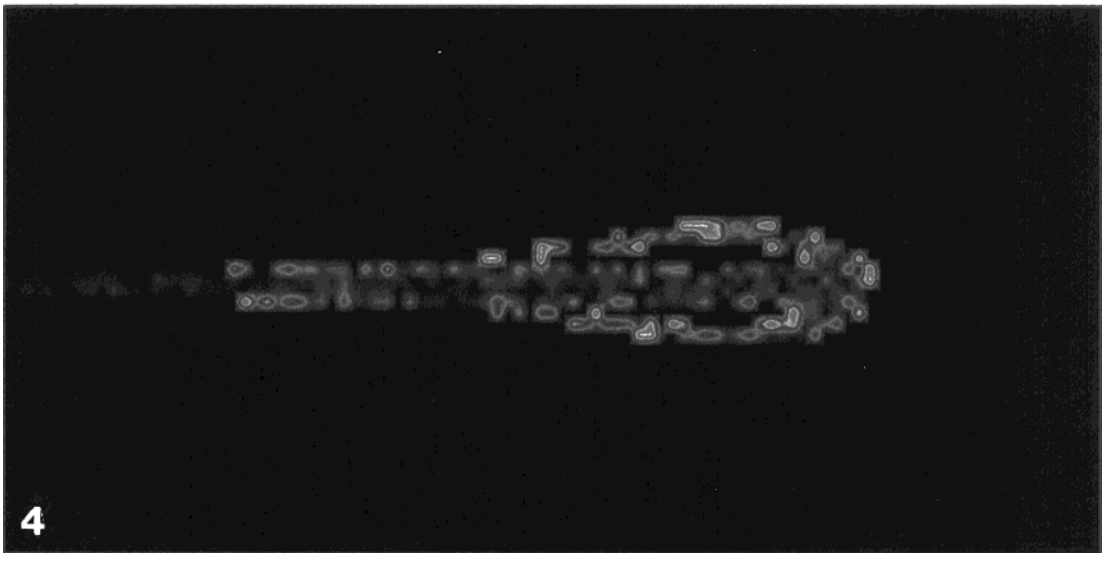
4

the two-phase fluid flow and therefore limits the effect of the local relative errors in the global behavior of the spray.

• In a second experiment, we consider small scale turbulence in the gas flow, which means that we take a nonzero diffusion coefficient D in the spray equation (2.9). Following [2], we know that the diffusion coefficient D may be computed in terms of the gas phase turbulent kinetic energy and the correlation time of the turbulence. More precisely, the diffusion in the spray equation accounts for the effects of the small scale turbulent structures in the gas velocity field while the large structures should be taken into account separately, for instance by means of a random component in the gas velocity. We thus need a model that gives the turbulent kinetic energy in the gas flow and the correlation time of the turbulence that should be considered to compute D.

Very few two-phase flow turbulence models are available. The presence of the dispersed phase should indeed influence the Kolmogorov cascade deeply: some characteristic length scales of the turbulence spectrum should be attenuated, which means that the presence of the particles induces a sink in some part of the energy spectrum, while small eddies are expected in the wake of the particles. Here, omitting the small scale turbulent structures produced by the Kolmogorov cascade, we may try to evaluate the small scale turbulent structures directly induced by the presence of the particles. Then, according to a dimensional analysis, we expect that the associated gas phase turbulent kinetic energy has the form

$$\mathscr{K}^{1/2} = C(1 - \alpha)\|\mathbf{u}_p - \mathbf{u}_g\| \text{ m/s},$$

where $1 - \alpha$ is the volume fraction of the dispersed phase, $\mathbf{u}_p$ is the mean velocity of the dispersed phase, $\mathbf{u}_g$ is the mean gas velocity, and C is an unknown coefficient. We shall take here

$$\mathscr{K} = (1 - \alpha)^2(\mathbf{u}_p - \mathbf{u}_g)^2, \tag{5.1}$$

where we set $C = 1$. Of course, more elaborate two-phase turbulence models that compare to experiments should be used but, as a first step toward more realistic computations, and in order to test the capabilities of our numerical method, we shall use such a simple law (5.1) in the sequel.

Indeed, at time $t = 0$, we set the internal kinetic energy E_k and the size S_k of each numerical particle injected as $E_k = 0$ m^2/s^2 and $S_k = 0.3$ mm. Here, the value of S_k is typical of the diameter of a liquid jet injected in a Diesel engine. The correlation time of the small eddies is taken as $t_d = 0.1(1/c(r))$ where $t_{drag} = 1/c(r) \simeq 2.5 \times 10^{-4}$ s is the ''capture time'' of a droplet. That is, we consider that the turbulent correlation time is smaller than the capture time. According to the discussion above, the specific turbulent kinetic energy of the small eddies is taken as $\mathscr{K}(\mathbf{x}) = 10^{-6}(\mathbf{u}_g(\mathbf{x}) - \mathbf{u}_p(\mathbf{x}))^2$ where $\mathbf{u}_p$ is the mean velocity of the droplets in the cell containing the point $\mathbf{x}$.

The shape of the spray and the velocity field of the gas are very similar to that obtained in the first experiment, with no turbulence modeling. The maximal velocity of the gas at time 1 ms is now 92.8 m/s, slightly smaller than in the first experiment. Actually, it seems important to us to remark that introducing the effect of the small scale turbulent structures introduces a new term of energy exchange between the two phases (compare Eqs. (2.7) and (2.11)). In other words, we may consider that some energy of the gas is transfered to the physical droplets of any given numerical particle.

Now, even if the general aspects of the two-phase fluid flow in the two experiments are very similar, we may look at the local relative error for the mass of the liquid between the two methods (see Fig. 4). This error still ranges in the interval [0, 1] and is quite important (compare with Fig. 3). Moreover we notice that the error is larger at the interface between the jet of droplets and the gas:

Then, though the shape of the spray is very similar to that obtained in the first experiment, the global relative error between the two methods is now 7% of the total mass injected and is thus quite important.

Finally, in our calculations the size of the numerical particles at the final time $t = 1$ ms ranges from 0.3 mm to 0.7 mm (see Fig. 5). The biggest numerical particles concentrate in the recirculation zone.

• In a third experiment, we consider a 2-m long and 1-m high channel containing air at a temperature of 300 K

FIG. 2. First experiment: chamber without turbulence modeling. Velocity of the gas at time $t = 1$ ms.

FIG. 3. First experiment: chamber without turbulence modeling. Comparison between the case where the trajectories of the particles are computed with exact integration formulas or by the finite differencing method. We plot in each cell the relative error $|m_1 - m_2|/\max(m_1, m_2)$ of the mass of liquid at time $t = 1$ ms, where the index refers to each calculation.

FIG. 4. Comparison between the first experiment, chamber without turbulence modeling, and the second experiment, chamber with turbulence modeling. We plot in each cell the relative error $|m_1 - m_2|/\max(m_1, m_2)$ of the mass of liquid at time $t = 1$ ms, where the index refers to each calculation.

at atmospheric pressure. The top and bottom boundaries of the channel are walls. The gas is injected on the left boundary of the channel with a velocity of 100 m/s and goes out through the right boundary of the channel. The mesh consists in square-shaped cells of size 2 cm.

At time $t = 0$, we begin the injection of non-vaporizing droplets. Here, the spray is polydisperse and the liquid is water. The injector is located at the center of the bottom wall. The direction of injection is 45° towards the left and the injection lasts for 0.1 s. The injection velocity is 100 m/s with a transverse component ranging in the interval $[-20\,\text{m/s}, +20\,\text{m/s}]$. The total mass injected is $M_T = 10$ Kg, and, setting here $K = 20$, $\Delta t_i = \Delta x/(KV)$ is the interval of time between the injection of two numerical particles. Following Dukowicz, the distribution of radii of the polydisperse spray is given by the exponential law

$$F(r) = \frac{3}{r_{DB}} \exp\left(-\frac{3r}{r_{DB}}\right), \tag{5.2}$$

where $r_{DB} = 5$ mm is the DeBroukier radius. Since we consider a finite number N of radii, we introduce the equiprobable family $(r_k)_{k=1,N}$ of radii where $r_k = (r_{DB}/3) \log[(N + 1)/(N + 1 - k)]$. In the limit where N goes to infinity the family $(r_k)_{k=1,N}$ reproduces the exponential law. However, the smallest radius of a numerical particle is here $r_1 = (r_{DB}/3) \log[(N + 1)(N)] \simeq r_{DB}/(3N)$ and it is necessary to bound N so that r_1 remains physically acceptable.

Let us make precise the numerical injection of droplets: the time interval between two injections is Δt_i and may differ from Δt. When $n\,\Delta t \le p\,\Delta t_i < (n + 1)\,\Delta t$ for some pair of integers (n, p) an injection of droplets occurs between t^n and t^{n+1}. We randomly chose a radius r_k with $1 \le k \le N$ and we decide that every droplet injected at time $p\,\Delta t_i$ has radius r_k. In order to determine the mass of the numerical particle injected at time $p\,\Delta t_i$ (or equivalently, the number of droplets taken into account in the numerical particle), we require that the mass flux of the liquid phase is constant: let us denote by $M(t)$ the total mass of liquid already injected at time t. If the injection process were continuous we could impose $M(t) = M_T t/T$, where M_T denotes the total mass of droplets injected at the end of the experiment. Here, the injection process is a discrete one and, in order to approximate the continuous law, the mass of particles injected at time $t = p\,\Delta t_i$ is given by the expression

$$m = \max\left\{M_T \frac{(p\,\Delta t_i)}{T} - M((p\,\Delta t_i)^-), 0\right\}, \tag{5.3}$$

and the total mass of droplets at time $(p\,\Delta t_i)^+$ is thus exactly $M_T(p\,\Delta t_i)/T$. With this algorithm, we inject a total mass $M_i = 9.99976$ kg instead of $M_T = 10$ kg, which proves the accuracy of the injection method. Finally, the injected mass of liquid is very important since it corresponds to 100 kg per second. This computation was performed in order to check the robustness of the whole numerical method.

Moreover, we take into consideration the possible break-up of the droplets thanks to a simple phenomenological model: let We denote the Weber number of a droplet with radius r_k,

$$\text{We} = \frac{\rho_g |\nabla \mathbf{u}|^2 r_k}{\sigma},$$

where ρ_g is the gas mass density at the position of the droplet, $\Delta\mathbf{u}$ the relative velocity between the droplet and the surrounding gas, and $\sigma = 0.073\,\text{kg/s}^2$ is the surface tension of water at a temperature of 300 K. When a droplet's Weber number becomes larger than a critical number (usually between 7 and 10), the droplet breaks up after a time interval that itself depends on the Weber number (see [16]). The result of the break-up is difficult to predict. However, we shall assume here that the droplets obtained from the breaking drop all have the same radius and a Weber number less or equal to 1. Of course a more realistic break-up model should be used in practical approximations but such a simplified model physically meaningful results to be obtained.

We show in Fig. 6 below the mass of the droplets inside the channel at time $t = 10$ ms. We observe the curvature of the droplet jet due to interaction with the gas velocity field. The velocity field at time $t = 10$ ms ranges between 2 and 170 m/s. It is shown in Fig. 7 below. We note that the presence of the droplets induces an important perturbation of the gas flow and a recirculation behind the liquid jet. Finally, the relative error between the droplet mass distributions, obtained thanks to the exact integration for-

FIG. 5. Second experiment: chamber with turbulence modeling. Size of the numerical particles at time $t = 1$ ms in each cell. The size of the numerical particles ranges from 0.3 mm to 0.7 mm.

FIG. 6. Third experiment: channel without turbulence modeling. Mass of the liquid in the channel at time $t = 10$ ms.

FIG. 7. Third experiment: channel without turbulence modeling. Velocity of the gas in the channel at time $t = 10$ ms.

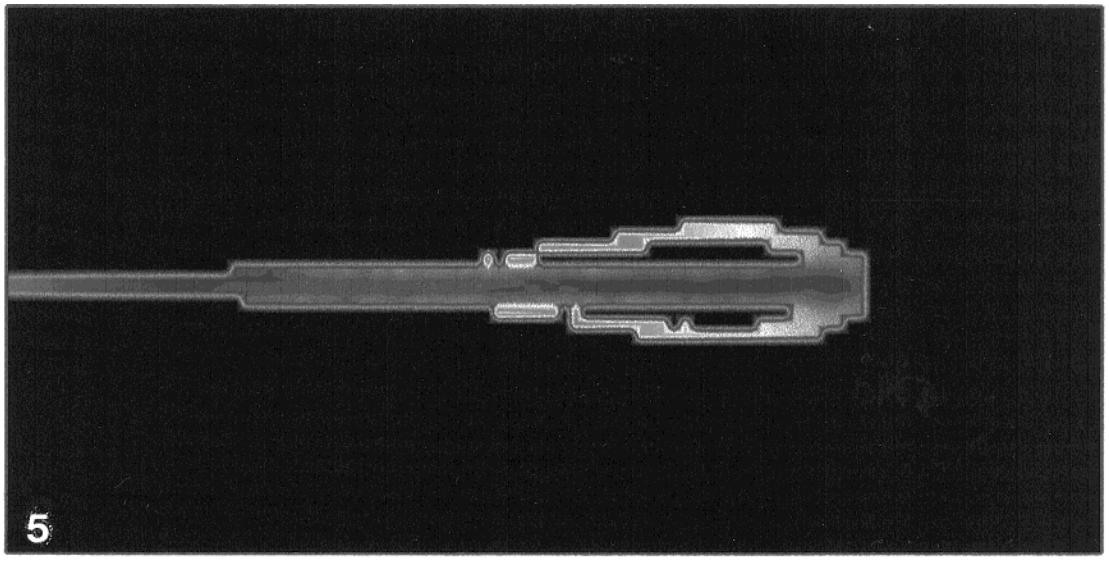
5

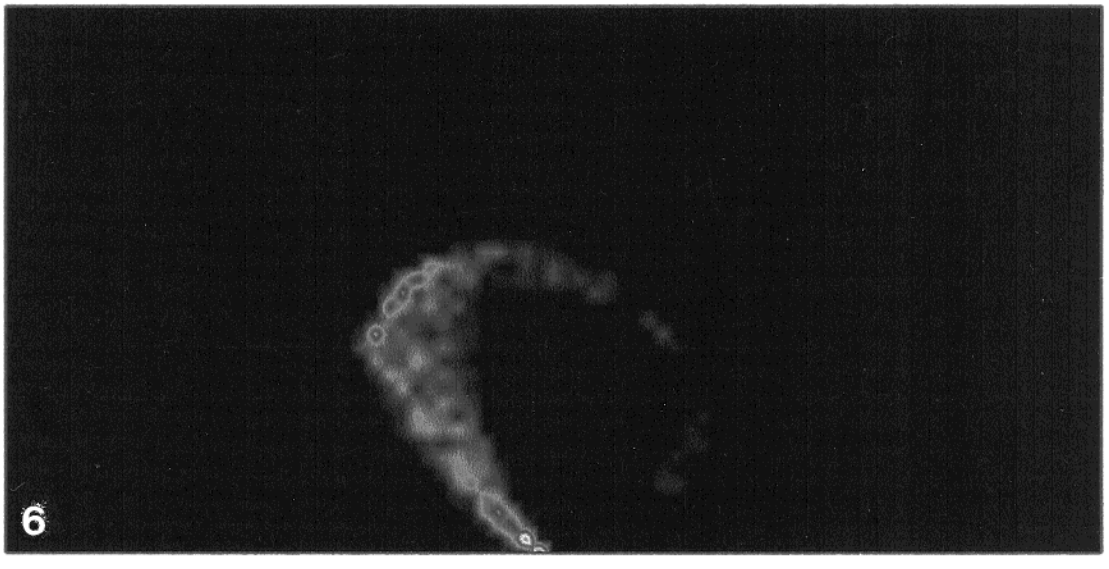
6

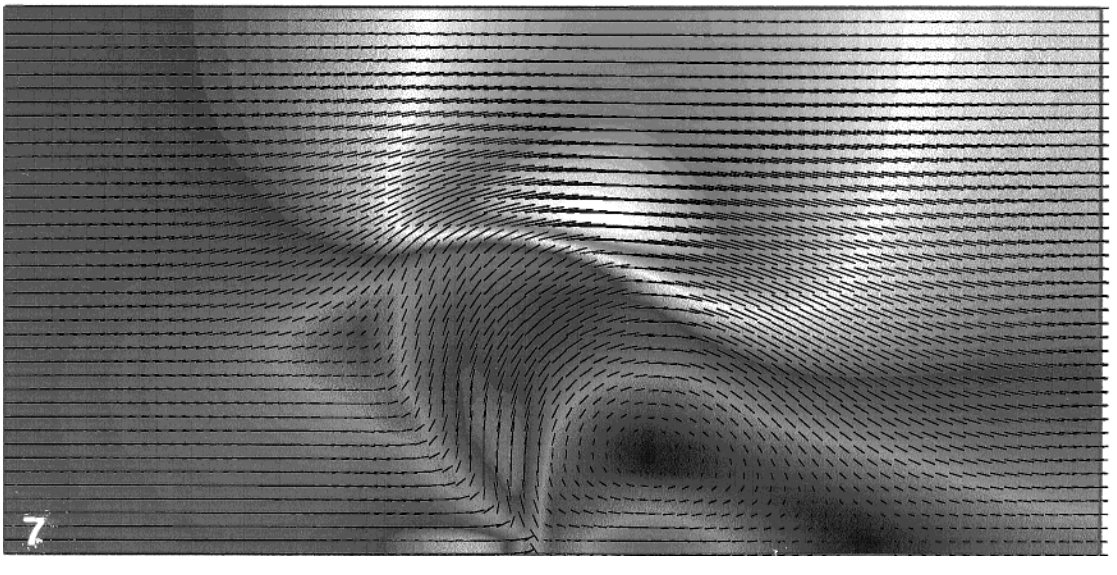
7

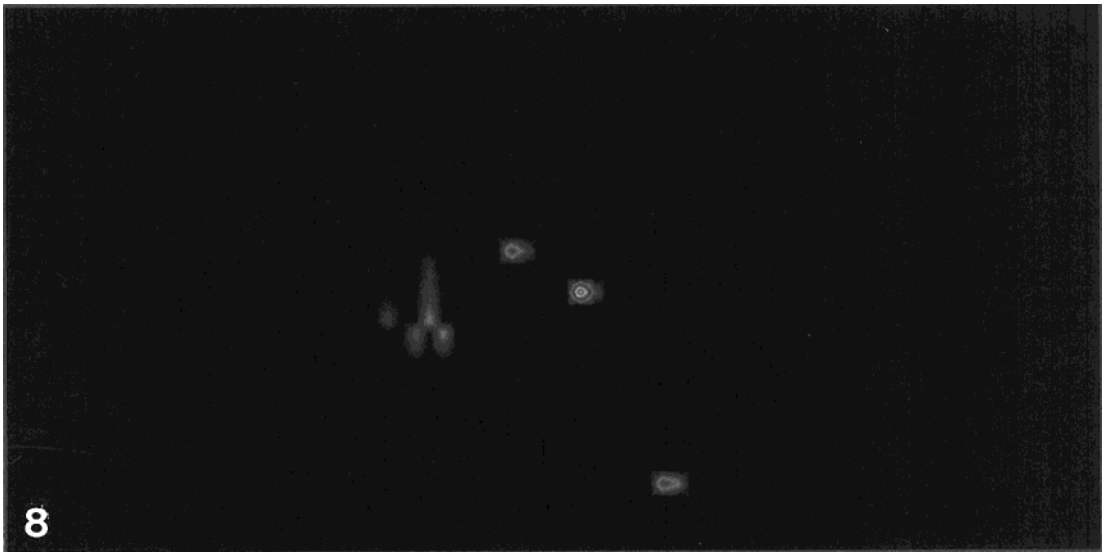

FIG. 8. Third experiment: channel without turbulence modeling. Comparison between the case where the trajectories of the particles are computed with exact integration formulas or by the finite differencing method. We plot in each cell the relative error $|m_1 - m_2|/\max(m_1, m_2)$ of the mass of liquid at time $t = 10$ ms, where the index refers to each calculation.

mula of the characteristics on the one hand and thanks to Euler's explicit first order integration formula on the other hand, is given in Fig. 8. Here the global relative error between the two methods is about 1.5% of the total mass injected.

6. CONCLUSION

The semi-fluid model allows us to gain more insight into the meaning of numerical particles in the domain of spray computation. We emphasize in this paper the general hypothesis that permit one to treat a numerical particle like a physical one. This is possible in this study first, since the velocity distribution of the droplets is assumed to be isotropic; second, because the spray obeys the linear transport equation (without collision terms); third, because the data on the gas flow are assumed to be constant in each cell of the computational domain when we compute the unknowns for the spray; and fourth, because we use the simple Stokes drag force. Finally, we insist on the fact that it is important to take into account the size of the numerical particles since this size is needed for the coupling between the two phases (see Remark 3.2 and Section 4.2).

We believe that using exact expressions for the characteristics of the droplets as well as taking into account the size of the numerical particle is important. Indeed, concerning the computation of the motion of the droplets, the use of a time step small enough that the particles' trajectory is accurately computed would dramatically increase the computational cost. For example, in the case of vaporizing sprays, it is never necessary with our method to use a subcycling of the timestep. The use of exact integrated expressions is therefore an important tool. However, we keep in mind that of course this may not be the main source of error when realistic two-phase fluid flows are computed. Indeed, one must first write more complex and realistic physical laws for the motion of the droplets, while we used in our computational examples the simplest ones.

Hence, this work is a first step toward a new numerical method for this type of systems but still much remains to be done: convergence of the method, comparison to fully kinetic models, and comparison with experiment. The numerical scheme introduced here for discretizing the semi-fluid model is elegant and efficient and therefore we believe that the numerical work presented here is a framework for future more complex physical descriptions of dispersed two-phase flows. In particular, the study of a two-phase flow turbulence model of $k - \varepsilon$ type is in progress.

A. APPENDIX: MATHEMATICAL RESULTS

This appendix is devoted to the derivation of some mathematical properties of the Fokker–Planck equation (2.9),

$$\partial_t f + \nabla_{\mathbf{x}} \cdot (f\mathbf{v}) + \nabla_{\mathbf{v}} \cdot (f\beta) + \partial_r(f\mathscr{R}) - \nabla_{\mathbf{v}} \cdot (D\nabla_{\mathbf{v}} f) = 0,$$

where $\beta = \beta(\mathbf{v}, r)$ and $D = D(r)$ are defined by (2.3) and (2.10), respectively. Its solution may be written explicitly as follows:

THEOREM A.1. (Solution of the Fokker–Plank Equa-

tion). *Let f_0 be given. The solution f of the Fokker–Planck equation* (2.9) *with initial data f_0 is written*

$$f(\mathbf{x},\mathbf{v},r,t) = (S_t f_0) = \frac{1}{|J_r(t)|} \int_{\mathbf{x}'}\int_{\mathbf{v}'} \mathscr{G}_{R^-}(\mathbf{X}^- - \mathbf{x}', \mathbf{V}^- - \mathbf{v}', t) f_0(\mathbf{x}', \mathbf{v}', R^-)\, d\mathbf{x}'\, d\mathbf{v}', \tag{A.1}$$

where $1/|J_r(t)|$ is the Jacobian $\partial(\mathbf{X}^-, \mathbf{V}^-, R^-)(t)/\partial(\mathbf{x},\mathbf{v},r)$ and

$$\mathscr{G}_r(\mathbf{x},\mathbf{v},t) = \frac{1}{(2\pi)^d\, \Delta_r^{d/2}(t)} \exp(-(a_r(t)\mathbf{x}^2 + 2h_r(t)\mathbf{x}\cdot\mathbf{v} + b_r(t)\mathbf{v}^2)/2\,\Delta_r(t)).$$

Here,

$$\begin{cases} a_r(t) = 2\int_0^t \psi_r^2(s)\, ds, & b_r(t) = 2\int_0^t \phi_r^2(s) \\ h_r(t) = 2\int_0^t \phi_r(s)\psi_r(s)\, ds, & \Delta_r(t) = a_r(t) - h_r(t) \end{cases} \tag{A.2}$$

where

$$\begin{cases} \psi_r(t) = \left(\dfrac{D(R(t;r,0))}{\eta_1^2(t)}\right)^{1/2} \\ \phi_r(t) = \left(\dfrac{D(R(t;r,0))\alpha_1^2(t)}{\eta_1^2(t)}\right)^{1/2}. \end{cases}$$

The numbers $\alpha_1(t)$ and $\eta_1(t)$ in the above expressions are the coefficients of the characteristics defined in Eq. (3.9).

Proof. Let us define the function $\tilde{f}$ by

$$\tilde{f}(\mathbf{x},\mathbf{v},r,t) = J_r(t) f(\mathbf{X}^+, \mathbf{V}^+, R^+, t). \tag{A.3}$$

where

$$J_r(t) = \exp\left(\int_0^t (\partial_r \mathscr{R} + \nabla_{\mathbf{v}}\cdot\beta)(R(s;r,0))\, ds\right). \tag{A.4}$$

A straightforward computation proves that $\tilde{f}$ is a solution of

$$(\partial_t \tilde{f})(\mathbf{x},\mathbf{v},r,t) = J_r(t) D(R(t;r,0))(\Delta_{\mathbf{v}} f)(\mathbf{X}^+, \mathbf{V}^+, R^+, t). \tag{A.5}$$

Thanks to Eq. (A.3) and the expression of the characteristics, the second term of Eq. (A.5) may be rewritten in terms of derivatives of $\tilde{f}$, so that

$$\partial_t \tilde{f}(\mathbf{x},\mathbf{v},r,t) = \frac{D(R(t;r,0))}{\eta_1^2(t)}(\alpha_1^2(t)\,\Delta_{\mathbf{x}}\tilde{f} - 2\alpha_1(t)(\nabla_{\mathbf{x}}\cdot\nabla_{\mathbf{v}})\tilde{f} + \Delta_{\mathbf{v}}\tilde{f})(\mathbf{x},\mathbf{v},r,t), \tag{A.6}$$

where α_1 and η_1 are the coefficients of the characteristics, defined in Eq. (3.9). Setting

$$\psi_r(t) = \sqrt{D(R(t;r,0))/\eta_1^2}, \quad \phi_r(t) = \sqrt{D(R(t;r,0))\alpha_1^2/\eta_1^2},$$

one recovers the expressions of ϕ_r and ψ_r defined in Theorem A.1. Hence, we are left to solve Eq. (A.6) in each of the d directions of $\mathbb{R}_x^d \times \mathbb{R}_v^d$, and we only need the following lemma:

LEMMA A.2. *Let $\phi(t)$ and $\psi(t)$ be two arbitrary functions of time. The solution in 1D of*

$$\begin{cases} \partial_t \mathscr{G} = \phi_r^2(t)\partial_{xx}\mathscr{G} - 2\phi_r(t)\psi_r(t)\partial_{xv}\mathscr{G} + \psi_r^2(t)\partial_{vv}G \\ \mathscr{G}(x,v,0) = \delta(x)\otimes\delta(v), \end{cases}$$

where δ denotes Dirac's δ function, is given by

$$\mathscr{G}(x,v,t) = \frac{1}{2\pi\,\Delta^{1/2}} \exp(-(a(t)x^2 + 2h(t)xv + b(t)v^2)/2\,\Delta(t))$$

with

$$\begin{cases} a(t) = 2\int_0^t \psi^2(s)\, ds, & b(t) = 2\int_0^t \phi^2(s)\, ds \\ h(t) = 2\int_0^t \phi(s)\psi(s)\, ds, & \Delta(t) = a(t)b(t) - h(t). \end{cases}$$

Proof. The proof of Lemma A.2 may be found in Chap. II of the article of S. Chandrasekhar (See [9]).

In other words, the solution $\tilde{f}(\mathbf{x},\mathbf{v},r,t)$ of (A.3) may be written in terms of a convolution operator in $(\mathbb{R}_{\mathbf{x}} \times \mathbb{R}_{\mathbf{v}})$,

$$\tilde{f}(\mathbf{x},\mathbf{v},r,t) = \int_{\mathbf{x}'}\int_{\mathbf{v}'} \mathscr{G}_r(\mathbf{x}-\mathbf{x}', \mathbf{v}-\mathbf{v}', r, t) f_0(\mathbf{x}', \mathbf{v}', r)\, d\mathbf{x}'\, d\mathbf{v}',$$

where $\mathscr{G}_r$ is defined in Theorem A.1. Thanks to Eq. (A.3), this means that the solution f of the Fokker–Planck equation (2.9) is given exactly by the expressions in Eq. (A.1). Note that the solution f is not written in terms of a convolution operator.

Now, let us identify the function $J_r(t)$. We note that the

characteristics defined in Eq. (3.8) may be written as the solution of the system of ODEs

$$\frac{d}{dt}\begin{bmatrix}\mathbf{X}_t\\ \mathbf{V}_t\\ R_t\end{bmatrix} = \mathbf{F}(\mathbf{X}_t, \mathbf{V}_t, R_t, t),$$

with obvious notations for $\mathbf{F}$. It is well known that the Jacobian $\partial(\mathbf{X}, \mathbf{V}, R)(t; s)/\partial(\mathbf{x}, \mathbf{v}, r)$ of the transformation $(\mathbf{x}, \mathbf{v}, r) \to (\mathbf{X}, \mathbf{V}, R)(t; s)$ equals 1 at $t = s$ and is a solution of the ODE

$$\frac{d}{dt}\left[\frac{\partial(\mathbf{X}, \mathbf{V}, R)(t; s)}{\partial(\mathbf{x}, \mathbf{v}, r)}\right] = \left(\begin{pmatrix}\nabla_{\mathbf{x}}\\ \nabla_{\mathbf{v}}\\ \partial_r\end{pmatrix}\cdot \mathbf{F}\right)\left[\frac{\partial(\mathbf{X}, \mathbf{V}, R)(t; s)}{\partial(\mathbf{x}, \mathbf{v}, r)}\right],$$

so that

$$\frac{\partial(\mathbf{X}, \mathbf{V}, R)(t; s)}{\partial(\mathbf{x}, \mathbf{v}, r)} = \exp\left(\int_s^t (\partial_r \mathscr{R} + \nabla_{\mathbf{v}}\cdot\beta)(R(\theta; r, s))\, d\theta\right).$$

Take $s = 0$: we obtain the expression (A.4) of $J_r(t)$. In other words, $1/J_r(t)$ is indeed the Jacobian associated with the flow of the reverse characteristics. This concludes the proof of Theorem A.1. ▮

ACKNOWLEDGMENTS

This work was supported by the Direction des Recherches of Etudes Techniques of the French Defense Ministry and the Pôle FIRTECH, Calcul Scientifique.

REFERENCES

1. F. A. Williams, *Combustion Theory*, 2nd ed., Benjamin–Cummings, Redwood City, CA, 1985.
2. J. F. Clouet and K. Domelevo, Solution of a kinetic stochastic equation modeling a spray in a turbulent gas flow, in *M3AS*, to appear.
3. P. D. Lax, A. Harten, and B. Van Leer, On upstream differencing and Godunov-type schemes for hyperbolic conservation laws, *SIAM Rev.* **25,** 35 (1983).
4. S. M. Deshpande, *Kinetic Theory Based New Upwind Methods for Inviscid Compressible Flows*, AIAA Paper 86-0275, American Institute of Aeronautics and Astronautics, New York, 1986.
5. B. Perthame, Boltzmann type schemes for gas dynamics and the entropy property, *SIAM J. Numer. Anal.* **27**(6), 1405 (1990).
6. C. Cercignani, *The Boltzmann Equation and Its Applications, Applied Mathematics*, Vol. 67, Springer-Verlag, Berlin/New York, 1988.
7. J. K. Dukowicz, A particle–fluid numerical model for liquid sprays, *J. Comput. Phys.* **35,** 229 (1980).
8. P. J. O'Rourke, Statistical properties and numerical implementation of a model for droplets dispersion in a turbulent gas, *J. Comput. Phys.* **83,** 345 (1989).
9. S. Chandrasekhar, Stochastic problems in physics and astronomy, *Rev. Mod. Phys.* **15**(1) (1943).
10. M. W. Reeks, On a kinetic equation for the transport of particles in turbulent flows, *Phys. Fluids A* **3**(3) (1991).
11. J. J. Monaghan and R. A. Gingold, Shock simulation by the particle method SPH, *J. Comput. Phys.* **52,** (1983).
12. S. Mas-Gallic and P. A. Raviart, A particle method for first-order symmetric systems, *Numer. Math.* **51,** 323 (1987).
13. B. Larrouturou, *On the Relation between Finite-Volume Simulations of Multi-dimensional and Multi-species Flow*, Internal Report, CERMICS, INRIA, Sophia-Antipolis, 06560 Valbonne, France.
14. P. L. Roe, Some contributions to the modelling of discontinuous flow, in *Lectures in Applied Mathematics*, Vol. 22, p. 163, 1985.
15. J. U. Brackbill, P. J. O'Rourke, and B. Larrouturou. On particle–grid interpolation and calculating chemistry in particle-in-cell methods, *J. Comput. Phys.* **109,** 37 (1992).
16. F. V. Bracco, Modelling of engine sprays, in *SAE 850394*, p. 144.